THE IDENTIFICATION AND LOCALIZATION OF THE ABELSON ONCOPROTEIN IN ZEBRAFISH, (*Danio rerio)*

A Thesis
By
Richard Charles de Triquet

Submitted to the Graduate School
Appalachian State University
In partial fulfillment of the requirements for the degree of
MASTER OF SCIENCE

December 2010
Department of Biology

THE IDENTIFICATION AND LOCALIZATION OF THE ABELSON ONCOPROTEIN IN ZEBRAFISH, (*Danio rerio)*

A Thesis
By
Richard Charles de Triquet
December 2010

APPROVED BY:

_____
Susan L. Edwards, Ph.D.
Chairperson, Thesis Committee

_____
Ted Zerucha, Ph.D.
Member, Thesis Committee

_____
Dru A. Henson, Ph.D.
Member, Thesis Committee

_____
Steven W. Seagle, Ph.D.
Chairperson, Department of Biology

_____
Edelma D. Huntley, Ph.D.
Dean, Research and Graduate Studies

Abstract

THE IDENTIFICATION AND LOCALIZATION OF THE ABELSON ONCOPROTEIN IN ZEBRAFISH, (*Danio rerio)*

(December 2010)

Richard Charles de Triquet, B.S., Belmont Abbey College

M.S., Appalachian State University

Chairperson: Susan L. Edwards, Ph.D.

The ubiquitously expressed Abelson oncoprotein (Abl) has multiple molecular functions, which affect homeostasis and cytoskeletal structuring of the cell. Mutation of the *Abl* gene is the causal event in several types of leukemia and is linked to the progression of certain lung and breast cancers. Despite extensive literature documenting the protein's function in humans and the recent explosion of cancer research using zebrafish, no research to date has investigated the existence of an Abl ortholog in *Danio rerio*.

We have sequenced a cDNA clone from *D. rerio* that demonstrates high identity to other vertebrate Abl proteins. In addition, we have investigated expression of the *abl* gene from 2-48 hours post fertilization (hpf) by *in situ* hybridization. The *abl* gene is expressed beginning at 12 hpf in the polster, a region of future brain development, and expression at this site continues through 48 hpf. Weaker expression is seen throughout the midsagittal line of the body at earlier stages and in the midsection and tail at later stages of the pharyngula period. Expression of the abl protein in zebrafish, examined by immunohistochemistry, is seen in the posterior blood island from 24-32 hpf.

Together, these results suggest that putative zebrafish abelson homolog has multiple functions in early development, aiding in the differentiation of neuronal cells in the central nervous system and also facilitating the production and differentiation of hematopoietic progenitor blood cells in the posterior blood island beginning at 24 hpf.

Dedication

To my grandfather, Thomas Joseph de Triquet

Acknowledgements

I would like to express gratitude for the countless people who have assisted me in the completion of this research. These people include my committee members: Dr. Sue Edwards, Dr. Ted Zerucha, and Dr. Dru Henson for invaluable mentoring and assistance. I also thank Brandon Carpenter for essential help with the *in situ* hybridization technique, Sal Blair for support, Dr. Guichuan Hou and Dr. Wayne Van Devender for microscopy assistance, Monique Eckerd for help raising zebrafish, and Kyle Nelson and Caroline Cochrane for help with molecular techniques. During my education at Appalachian State University, I have been supported by a National Science Foundation: S-Stem scholarship, a graduate teaching assistantship, out of state graduate assistant tuition remissions, and an office of student research travel grant. Finally, I want to recognize my family for all of the tangible, and more importantly, the intangible support throughout my graduate education.

Table of Contents

Abstract iv

Dedication vi

Acknowledgments vii

List of Tables ix

List of Figures x

Introduction 1

Methods 12

Results 18

Discussion 22

Tables 27

Figures 28

References 44

Biographical Sketch 52

List of Tables

Table 1 Primers used for cDNA clone sequencing 27

List of Figures

Figure 1 The Philadelphia chromosome 28

Figure 2 Isoforms of the Abelson protein 29

Figure 3 The molecular activity of the Bcr-Abl tyrosine kinase 30

Figure 4 Inactive and active conformations of c-Abl 31

Figure 5 Nucleotide and deduced amino acid sequence of the putative *Danio rerio* Abelson 1 ortholog.....32

Figure 6 Amino acid sequence alignments of Abl1 orthologs and Bcr-Abl.....35

Figure 7 Phylogenetic tree of Abl1 orthologs and Bcr-Abl 37

Figure 8 Whole-mount *in situ* hybridization of *abl* expression at 2 and 12 hpf 38

Figure 9 Whole-mount *in situ* hybridization of *abl* expression from 18-32 hpf.....39

Figure 10 Whole-mount *in situ* hybridization of *abl* expression at 36 and 48 hpf 40

Figure 11 Whole-mount *in situ* hybridization negative controls 41

Figure 12 Whole-mount immunohistochemistry of abl expression.....42

Figure 13 Western blot.....43

Introduction

The Abelson (Abl) oncoprotein performs an array of cellular functions that affect the homeostatic characteristics of the cell. Although the protein is ubiquitous in all cell types (Sirvent, Benistant, & Roche, 2008), its most deleterious effects can be found within blood cells where it was discovered 50 years ago. In 1960, Peter Nowell and David Hungerford discovered a shortened chromosome 22 that was consistently found within the blood cells of patients diagnosed with chronic myeloid leukemia (CML) (Nowell & Hungerford, 1960). The disease causes increased proliferation of the myeloid cell lineage (Daley, Vanetten, & Baltimore, 1990), which includes granulocytic cells and monocytes (Parham, 2005). The discovery of a consistent genetic mutation linked to a specific oncogenic progression was the first of its kind and spawned decades of intensive research focused on discovering the molecular activity of the Abl protein.

Investigations by Janet Rowley in 1973 established that the shortened chromosome 22 found in CML patients was the result of a translocation with chromosome 9 (Rowley, 1973), while later studies confirmed that this reciprocal translocation involved the *Abl* gene on the long arm of chromosome 9 and the *Bcr* gene on the long arm of chromosome 22 (see Figure 1) (Shtivelman, Lifshitz, Gale, & Canaani, 1985). The mutated chromosome was named the Philadelphia chromosome after the city of its discovery (Druker, 2008), and contains the *Bcr-Abl* fusion gene, which produces a constitutively active fusion kinase. It is

produced in a hematopoietic stem cell (HSC) and after HSC division it can be found in myelocytes, megakaryocytes, erythrocytes, and small lymphocytes (Daley et al., 1990). Bcr-Abl causes malignant transformation of HSCs and hematopoietic progenitor cells through altered cellular adhesion, inhibition of apoptosis, and stimulation of mitogenic pathways resulting (Daley et al., 1990; Deming et al., 2004; Gross & Ren, 2000; McGahon et al., 1997). This specific fusion kinase is present in >95% of patients with CML, ≈20% of adult acute lymphoblastic leukemia patients (Gross & Ren, 2000; Kurzrock, Kantarjian, Druker, & Talpaz, 2003; Reinhold, Hennig, Leiblein, Niederwieser, & Deininger, 2003; Shtivelman et al., 1985), and ≈5% of pediatric acute lymphoblastic leukemia patients while fusion of *Abl* to the *Tel* gene results in T-cell acute lymphocytic leukemia (Srinivasan, Sims, & Plattner, 2008). Major headway was made in 2001 when the Food & Drug Administration approved the use of a tyrosine kinase inhibitor that was able to shut down Abl kinase activity, effectively reversing the progression of CML (Druker, 2008).

Despite this momentous medical triumph, a subset of patients still develop resistance to the kinase inhibitor and all patients harbor a persistent population of Bcr-Abl positive blood cells within the major adult site of hematopoiesis: the bone marrow (Jin et al., 2009; Reinhold et al., 2003). HSCs in inactive states reside within the endosteal niche of the bone marrow and adhere to thrombopoietin producing osteoblasts cells (Yoshihara et al., 2007). When stimulated, these cells can migrate to microvascular subregions immediately adjacent to osteoblasts where stromal cell derived factor-1 chemokines are expressed (Sipkins et al., 2005). These vascular subregions can harbor residual leukemic cells, including Bcr-Abl positive cells, following clinical treatment suggesting that this microenvironment stimulates anti-apoptotic characteristics in cells residing there (Sipkins et al., 2005). For these reasons,

investigations in *Homo sapiens*, *Mus musculus*, and *Drosophila* have continued with the ultimate goal of fully understanding the normal and altered molecular activity of the Abl kinase within all types of cells, especially hematopoietic cells.

The Abl tyrosine kinase

The *Abl* gene encodes for a non-receptor tyrosine kinase that is localized within the nucleus and cytoplasm (Plattner, Kadlec, DeMali, Kazlauskas, & Pendergast, 1999; Sirvent et al., 2008; Sun et al., 2000; Wetzler et al., 1993). It represents one of 32 different non-receptor tyrosine kinases in the human kinome that are stimulated by cytokines, growth factors, and receptors (Sirvent et al., 2008). In humans, there are four major Abl isoforms that are similar in structure to Bcr-Abl, v-Abl and the related c-Src tyrosine kinase (see Figure 2) (Sirvent et al., 2008). The Abl1a and Abl1b isoforms (c-Abl) and the Abl2a and Abl2b isoforms (Arg1a and 1b) have a molecular weight of 145 kilodaltons (kD). Following the N-terminus, all isoforms contain a Cap region, the SH3, SH2, and Kinase domains (Koleske et al., 1998; Plattner et al., 1999; Sirvent et al., 2008). Abl1a and Abl2b isoforms possess N-terminal myristolation (Sirvent et al., 2008). All isoforms contain a polyproline (PXXP) rich region following the Kinase domain, which interacts with the Abl SH3 domain when inactive and with the SH3 domain of other proteins when active, thus aiding in protein interactions (Plattner et al., 1999; Sirvent et al., 2008). Both Abl1 isoforms contain nuclear localization signals and a DNA binding domain essential for nuclear functions (Plattner et al., 1999; Sirvent et al., 2008). Abl2 isoforms contain the DNA binding domain but are absent of nuclear localization signals indicative of cytoplasmic function (Plattner et al., 1999; Sirvent et al., 2008). For all isoforms, the remaining portion of the C-terminus end contains a

globular actin (G-actin) binding domain, a filamentous actin (F-actin) binding domain, and a nuclear export signal essential for cytoplasmic migration (Plattner et al., 1999; Sirvent et al., 2008).

The v-Abl isoform (Abelson murine leukemia virus) is a cellular homologue of Abl1 and contains an altered N-terminus with deletion of the SH3 domain (Daley et al., 1990; Sirvent et al., 2008). The mutated form of the Abl kinase contains the addition of the Bcr region adjacent to the SH3 domain causing the deletion of the N-terminus Cap region and myristolation site in Abl1b and Abl2b isoforms (Sirvent et al., 2008). Bcr-Abl proteins with weights of 190, 210, and 230 kD occur with breaks occurring at different exons of the *Bcr* gene prior to translocation (Kurzrock et al., 2003). These isoforms are strictly localized to the cytoplasm and display increased activity (Sirvent et al., 2008).

Activity of the Abelson tyrosine kinase is contingent on binding with substrate proteins, which facilitates phosphorylation of those substrates. This action occurs within the Kinase domain of Abl through transfer of a terminal phosphate group from adenosine triphosphate (ATP) to a tyrosine residue on the substrate protein (see Figure 3) (Sirvent et al., 2008). Phosphorylation by Abl occurs through numerous partners allowing it to propagate a suite of signals (Druker, 2008). The type of signal depends on the specific isoform and the cellular location. Similar to other kinases, Abl configuration and activity is tightly regulated (Plattner et al., 1999); regulation is achieved by interaction of the SH2, SH3, and Kinase domains to maintain the Abl in the closed inactive conformation (see Figure 4) (Sirvent et al., 2008). The N terminus interacts with a pocket on the C-lobe of the kinase domain to strengthen the closed shape (Sirvent et al., 2008). Consequently, loss of the N-terminus results in constitutive activation (Kurzrock et al., 2003). Phosphorylation at the activation

loop (Y245) and the linker region (Y412) effectively causes the protein to assume an open conformation and become active (see Figure 4) (Kurzrock et al., 2003). Normal phosphorylation at these sites is controlled by motifs in the N-terminal of Abl so loss of this region to Bcr fusion causes altered phosphorylation and constitutive activation (Kurzrock et al., 2003).

Cellular functions

Abl isoforms display different molecular functions in both the nucleus and cytoplasm and can shuttle between the nucleus and cytoplasm for activity in multiple locations (Sirvent et al., 2008). Within the nucleus, Abl1 isoforms respond to DNA damage through a variety of proteins including P75, P73 P53, STAT3, and HS1 (Agami, Blandino, Oren, & Shaul, 1999; Gong et al., 1999; Lapetina, Mader, Machida, Mayer, & Koleske, 2009; Sirvent et al., 2008; Srinivasan et al., 2008; Sun et al., 2000). When interacting with P53 or P73 tumor suppressor proteins, Abl1 can halt the cell cycle at the G1 phase and initiate apoptosis (Agami et al., 1999; Sun et al., 2000). Alternatively, it can promote G1 to S phase progression and proliferation in breast cancer cells through STAT3 (Srinivasan et al., 2008).

Cytoplasmic functions are involved with cytoskeletal structure, an important feature in regulation of cell shape, cell movement, and cell-to-cell interactions. Cytoplasmic Abl activation can promote DNA synthesis, F-actin assembly and receptor trafficking (Sirvent et al., 2008). In other cells, the proliferative capacity of Abl is induced by platelet-derived growth-factor (PDGF) and directly activated by phosphorylation at Y412 and Y245 through the Src family kinases (Plattner et al., 1999; Sirvent et al., 2008; Srinivasan & Plattner, 2006; Srinivasan et al., 2008). Activation triggers Abl association with cortactin and F-actin

resulting in cortactin phosphorylation and F-actin polymerization (Plattner et al., 1999). The resulting F-actin polymerization is required for proper cytoskeletal structuring of lamellipodia, filopodia, dorsal ruffles, and neurite extensions (Boyle, Michaud, Schweitzer, Predki, & Koleske, 2007; Plattner et al., 1999; Sirvent et al., 2008). Circular dorsal ruffling, a structural feature linked to macro-pinocytosis and cell migration is commonly observed in leukocytes (Plattner et al., 1999; Sirvent et al., 2008). In addition, dorsal ruffle formation by Abl activation can also be linked to increased invasion of several breast cancer cell lines (Srinivasan & Plattner, 2006; Srinivasan et al., 2008).

Within specific leukocyte lineages Abl isoforms have been implicated in stimulation proliferation and apoptotis. The B cell inhibitory Fc receptor is dependent upon Abl1 signaling in the stimulation of B-cell apoptosis (Tzeng, Bolland, Inabe, Kurosaki, & Pierce, 2005). In T cells, receptor stimulation results in activation of Abl kinases leading to IL-2 production and T cell proliferation (Zipfel, Zhang, Quiroz, & Pendergast, 2004). Abl1 is also required for actin polymerization and lamellipodial spreading at the immune synapse in T and B cells, a feature necessary for engagement of the T and B cell receptor to antigens, cell-to-cell contact, and effective T-cell migration (Huang et al., 2008; Lapetina et al., 2009).

Abl's role in various hematopoietic processes is evident by the malignant transformation of HSCs containing the Bcr-Abl protein. Normal forms of Abl are also involved with a number of homeostatic processes within the cell that affect the survival of the cell and cytoskeletal structure allowing interaction with the extracellular environment. These functions raise many questions concerning the role of Abl in the migration, structure, and differentiation of diverse cell types during embryonic development. Despite a multitude

of documented Abl functions, there are still large gaps of missing information and no research to date has been published linking the Abl tyrosine kinase and zebrafish.

Zebrafish

The Abl functions discussed thus far have been researched in humans and established animal models, but we aim to investigate the possible functions in *Danio rerio*. The zebrafish, a valuable model of early development, hematopoiesis, and cancer is an ideal candidate for modeling human disease based on its small size, ease of breeding, ex-utero development of embryos and transparency of those embryos (Meeker & Trede, 2008; Yoder, Nielsen, Amemiya, & Litman, 2002). Most importantly, the large number of orthologous genes that zebrafish share with mice and humans allow further investigation of *Abl* functioning. One area of research that still deserves greater attention is the role that Abl plays in embryonic development. Abl1 and Abl2 double knockout in mice proves lethal at embryonic day 9, demonstrating that the proteins are essential during early development (Koleske et al., 1998). Abl has also been implicated in the development of axonal outgrowths in *Drosophila* (Plattner et al., 1999) and proper construction of the central nervous system in *Mus musculus* (Koleske et al., 1998); thus, it is possible that Abl may be involved with zebrafish neurogenesis. It is also relevant to examine the role of Abl in the early establishment of hematopoiesis. We know that mutation can cause established hematopoiesis to go awry. However, possible functions the kinase may have in the establishment of definitive hematopoiesis and its role in early hematopoietic progenitor cells is not known.

Hematopoiesis

Zebrafish are known to have many hematopoietic homologies with humans due to the evolution of the adaptive immune system prior to the divergence of fish from other vertebrates (Meeker & Trede, 2008). Accordingly, zebrafish are known to produce nearly all of the same blood cell types as humans with the main difference between the two species being the sites of blood cell maturation during development (Meeker & Trede, 2008). Currently, there are many blood related diseases being modeled by zebrafish: MOZ/TIF2-induced acute myeloid leukemia (Zhuravleva et al., 2008), heat shock induced T-cell lymphoma (Feng et al., 2007), Notch1-induced T-cell leukemia (Chen et al., 2006; Sharma et al., 2006), Myc-Induced T Cell leukemia (Langenau et al., 2002), and B-cell chronic lymphocytic leukemia (Auer, Riaz, & Cotter, 2007). This is possible due to many hematopoietic homologies. One identifying characteristic of vertebrate hematopoiesis is the presence of HSCs within various anatomical regions during different waves of blood cell production (Jin et al., 2009).

During early development, vertebrate hematopoiesis progresses in successive waves that occur in several different organs (Murayama et al., 2006). The first wave, or primary wave, gives rise to the most immediately needed blood cell types both developing in the yolk sac: erythrocytes containing embryonic globin proteins (Davidson & Zon, 2004; Kalev-Zylinska et al., 2002) and macrophages (Samokhvalov, Samokhvalova, & Nishikawa, 2007; Willett, Cortes, Zuasti, & Zapata, 1999; Zapata, Diez, Cejalvo, Frias, & Cortes, 2006). These two cell types are essential in oxygenating and remodeling embryonic tissue (Bertrand et al., 2007). Appearance of these blood cells in zebrafish coincides with the initiation of circulation at 24 hours post fertilization (hpf) (Isogai, Horiguchi, & Weinstein, 2001). Based

on these findings, the yolk sac has been regarded as a primitive hematopoietic organ, not capable of producing definitive blood cell types such as lymphocytes and myeloid cells.

But recent studies have also shown that this region can also contain progenitor cells, which differentiate to produce definitive blood cell types in hematopoietic colony assays (Orkin & Zon, 2008; Samokhvalov et al., 2007; Weissman, 1978). Other studies have shown that cells migrating from the yolk sac express *Runx1* which codes for a transcription factor essential for HSC emergence, when the yolk sac is the sole hematopoietic site (Bertrand et al., 2007; Samokhvalov et al., 2007). These cells can be traced and later contribute to definitive hematopoiesis; about 1-10% of adult HSCs have origins in the yolk sac in murine studies (Samokhvalov et al., 2007). Studies in zebrafish show that hematopoietic cells arising from the yolk sac generate an erythromyeloid progenitor (EMP) that migrates to the aorta-gonad mesonephros (AGM) region (Bertrand et al., 2007). HSCs also emerge directly in the AGM, (Jin et al., 2009; Orkin & Zon, 2008; Samokhvalov et al., 2007) and the ventral wall of the dorsal aorta shortly after the onset of circulation and express the HSC associated genes, *c-myb* and *runx1* (Bertrand et al., 2007; Davidson & Zon, 2004; Jin et al., 2009; Murayama et al., 2006). It is commonly held that definitive hematopoiesis begins with HSC production in the AGM and their migration to later hematopoietic sites (Bertrand et al., 2007; Murayama et al., 2006; Murry & Keller, 2008), where they produce a diversified blood cell repertoire (Bertrand et al., 2007; Murayama et al., 2006). EMPs in the zebrafish AGM do migrate to a region in the tail where they later produce erythroid and myeloid cells (Bertrand et al., 2007). But, HSCs in the AGM are not totally dormant and do give rise to myeloid cells in zebrafish between 28-48 hpf suggesting that the AGM is a hematopoietic site which does

contribute to the blood cell repertoire and is more than just a transition zone for HSCs on their way to subsequent niches (Bertrand et al., 2007; Jin et al., 2009).

HSCs in zebrafish migrate to the ventral tail region from 24-48 hpf and display the presence of several genes including *c-myb*, *runx1*, *lmo*, and *mpx*, which are all known to participate in hematopoiesis within humans (Bertrand et al., 2007); in addition, these cells also display the presence of the transcription factor pu.1, a powerful factor essential in myeloid and lymphoid cell development (Hsu et al., 2004; Ward et al., 2003). This region termed the posterior blood island (PBI) is also referred as caudal hematopoietic tissue (CHT), and the intermediate cell mass (ICM) at earlier stages. The fetal liver within humans and the PBI within zebrafish serve as an intermediate site of hematopoiesis during development following cell production in the AGM (Orkin & Zon, 2008). In zebrafish, HSCs in this region migrate from the PBI to the kidney, which is the adult site of hematopoiesis (Orkin & Zon, 2008). It is not known whether this type of HSC migration occurs in humans, but HSCs begin to appear in the fetal liver and bone marrow at roughly the same time (Orkin & Zon, 2008). HSCs in the fetal liver differentiate into common myeloid progenitors (CMPs) and common lymphoid progenitors (CLPs), but display less restrictive lineage commitment (Jin et al., 2009). The CLPs in this region can give rise to lymphoid cells and macrophages (Mebius et al., 2001). It is probable that some HSCs from the liver migrate to the marrow and that HSCs emerge in the marrow de novo (Orkin & Zon, 2008).

The shifting location of HSCs throughout development has consequences on the their differentiation repertoire and potential due to niche influence on HSC (Jin et al., 2009). Although the precise origin of HSCs leading to definitive hematopoiesis is debated, it is known that cells with progenitor capacity can be found in the yolk sac, the AGM, fetal liver,

and bone marrow of humans. In zebrafish, progenitor cells can be observed in the yolk sac, AGM, PBI, and kidney. The presence of hematopoietic cells within multiple regions at various stages in development is consistent with the notion that the hematopoietic potential of progenitor cells changes as the primary site of hematopoiesis shifts.

The presence of similar blood cells and genes and their development emphasize hematopoietic homologies present in zebrafish. These conserved hematopoietic mechanisms allowing a variety of blood based cancers to be modeled in the organism supporting the possibility of finding an active *Abl* gene in the fish. Moreover, the *Abl* gene is evolutionarily conserved across disparate organisms including nematodes, flies, mice and humans (Henkemeyer, West, Gertler, & Hoffmann, 1990).

Purpose of study

The long-range goal of this research was to characterize the expression of the putative Abelson gene and protein during early embryonic development in zebrafish. Our working hypothesis was that an ortholog of the human Abl protein is active in zebrafish functioning in multiple aspects of hematopoiesis including cell growth, proliferation, and migration. The three main objectives of this research were to clone and sequence cDNA obtained from *D. rerio* tissue homologous to human *Abl*, examine expression of the *Abl* mRNA in *D. rerio* by whole-mount *in situ* hybridization (ISH) from 2-48 hpf, and determine the temporal and spatial expression of the Abl protein during early hematopoiesis by whole-mount immunohistochemistry (IHC) and western blot techniques.

Methods

Zebrafish husbandry and embryo collection

Zebrafish were housed in a Z-Mod system (Aquatic Habitats) and maintained at 28°C on a 16 hour light / 8 hour dark cycle. Breeding of adult AB line fish was facilitated in specialized mating chambers, which allowed for subsequent embryo collection. Embryos were staged according to a staging series based on morphological features (Kimmel, Ballard, Kimmel, Ullmann, & Schilling, 1995) and fixed overnight in 4% paraformaldehyde (PFA) prior to de-chorionation and dehydration in methanol for use in ISH and IHC. For western blot studies, embryos staged at 18, 24, 32, and 36 hpf were snap frozen in liquid nitrogen and stored at -80°C. The Appalachian State University IACUC approved all procedures involving the use of zebrafish.

cDNA clone sequencing and sequence analysis

A *Danio rerio* cDNA clone was purchased through Open Biosystems (clone ID: 3857626, Accession: EB951650). The gene was subcloned into a pSport1 vector and propagated in the DH5α bacterial strain. Plasmid DNA for sequencing reactions and ISH was isolated by a PureYield Plasmid Maxiprep System (Promega, Madison, WI). Primers were designed by MacVector11.0 and ordered (Eurofins MWG Operon, Hunstville, AL) for use in sequencing reactions (see Table 1). Cornell Life Sciences Core Laboratories Center and

Mount Desert Island Biological Station performed sequencing reactions. The obtained sequence was translated with the ExPASy proteomics server (http://ca.expasy.org/tools/dna.html) and aligned with other sequences using ClustalW2 (http://www.ebi.ac.uk/Tools/ clustalw2/index.html). Phylogenetic tree analysis was completed with Phylogeny.fr (http://www.phylogeny.fr/) using MUSCLE 3.7 for multiple sequence alignment, GBlocks 0.91b for alignment refinement, PhyML 3.0 aLRT for phylogeny, and TreeDyn 198.3 for tree rendering (Dereeper et al., 2008). Amino acid sequences from Abl1 orthologs, predicted Abl1orthologs, and Bcr-Abl were used for multiple sequence alignments and phylogenetic tree construction: translation of *Danio rerio* cDNA clone (EB951650), predicted *Danio rerio* v-Abl1 homolog (XP_001337899.1), *Homo sapiens* (NP_005148.2), *Mus musculus* (NP_001106174.1), *Rattus norvegicus* (ABC46642.1), Bcr-Abl fusion kinase (ABX82702.1), *Pongo abelii* (XP_002833232.1), *Equus caballus* (XP_001917300.1), *Xenopus (Silurana) tropicalis* (XP_002936228.1), *Strongylocentrotus purpuratus* (XP_001203875.1).

Whole-mount *in situ* hybridization

Plasmid DNA was linearized separately by either a Not1 or Sal1 restriction digest, purified with a DNA clean and concentrator kit (Zymo Research, Orange, CA), its concentration determined by NanoDrop, and checked for linearization by gel electrophoresis. A digoxigenin (DIG) RNA labeling Kit was used for RNA labeling with DIG-UTP by in vitro transcription using SP6 and T7 RNA Polymerase (Roche, Indianapolis, IN). Plasmid DNA cut with Sal1 was transcribed with SP6 promoters for Antisense (AS) experimental probes. Plasmid DNA cut with Not1 was transcribed using T7 promoters for Sense (S)

negative control probes. The transcription reaction contained 10x transcription buffer, DIG labeled nucleotides, RNAse inhibitor, T7 or SP6 polymerase, 1ug of cut plasmid DNA, and DEPC-H20 to bring to a 20 ul volume. These reactions were incubated at 37°C for 2 hours, template DNA was removed by incubation with DNAse I recombinant (Roche, Indianapolis, IN) at 37°C for 30 min. Transcribed probes were then precipitated overnight using 4M Lithium Chloride and 100% Ethanol. Efficiency of DIG-RNA transcription was checked by gel electrophoresis and concentration of RNA probe determined by NanoDrop.

Within 24-well plates, embryos were progressively rehydrated to 0.1% PBS Tween (PBT), permeabolized with Proteinase K at stage dependent times according to (Thisse & Thisse, 2008) and incubated in 4% PFA for 20 min. Embryos were then pre-hybridized at 70°C for 5 hr in hybridization mix (HM) at a final pH of 6.2 containing 50% formamide, 5xSSC, 50 ug/ml heparin, 500 ug/ml torula yeast, and 0.1%Tween. After pre-hybridization, embryos were incubated at 70°C overnight in HM containing 50 ng of AS or S probe per well respectively for experimental and negative controls. The following day, embryos were washed with 2X and 0.2X SSC, progressively brought to PBT, and then incubated in BSA:PBT:5% sheep serum at room temperature for 1 hour. Embryos were then incubated at 4°C overnight with an anti-DIG-alkaline phosphatase antibody (α-DIG-AP) (Roche, Indianapolis, IN) at a 1:2000 concentration. The next day, embryos were washed with PBT and any bound α-DIG-AP antibodies were visualized by a staining reaction with NBT/BCIP color development substrate. A Meiji compound microscope fitted with a Leica DFC320 digital camera and the Leica Application Suite Version 3.3.1 program was used for picture acquisition. Images were compiled using Microsoft PowerPoint 2008 for Mac.

Whole-mount immunohistochemistry

Fixed, staged embryos were rehydrated to PBS and non-specific binding sites were blocked by incubation in blocking solution at room temperature for 30 min. Blocking solution contained 50 ul/ml Normal Goat Serum (NGS), 6.7 ul/ml triton, and 940 ul/ml PBS. Embryos were incubated with 1:100 primary antibody at 4°C overnight; negative controls were kept in blocking solution at 4°C during that time. The sc-131 primary antibody (Santa Cruz Biotechnology, Santa Cruz, CA) used in protein studies was a polyclonal rabbit antibody specific to the kinase domain of human Abl1. The following day, embryos were washed with 0.1% PBS triton and incubated for 1 hour at room temperature with 1:1000 goat-α-rabbit-AP antibody (Bio-Rad, Hercules, CA). Bound antibody was stained by NBT/BCIP reaction and visualized by techniques used in ISH.

K562 cell culture and whole cell extract

K562 cells, a CML cell line containing the Bcr-Abl fusion kinase (Amar et al., 1992), were incubated in filter sterilized Iscove base media containing heat inactivated fetal calf serum (Atlanta Biologicals, Lawrenceville, GA) sodium-pyruvate, L-glutamine, and penicillin-streptomycin solution. Cells were incubated at 37°C at 5% CO2. Approximately 2 x 10^7 cells were collected and re-suspended in an eppendorf tube containing 500 ul of PBS. Cells were spun for 10 s at 13,200 RPMs. PBS was aspirated and cell pellet was re-suspended in 150 ul of freeze-thaw buffer (F-T) containing 250M tris-HCl at pH8, 10mM dithithreitol, and 15% glycerol. Cells in F-T buffer were frozen in liquid nitrogen then thawed in a 37°C water bath and repeated for a total of four freeze thaw events. The sample was centrifuged at 10,000 RPM at 4°C for 5 min and the supernatant containing whole cell

extract was quantified for protein concentration using a bicinchoninic acid protein assay kit (Thermo Fisher Scientific, Rockford, IL).

Western blot

Snap frozen zebrafish embryos were homogenized in a buffer solution; homogenization buffer had a final pH of 7.8 and contained sucrose, tris base, 100mM EDTA, phenylmethylsulfonyl fluoride and protease inhibitor cocktail. Homogenized samples were centrifuged at 14,000 RPM at 4°C for 10 min and supernatants were collected for protein quantification according to a bicinchoninic acid protein assay kit (Thermo Fisher Scientific, Rockford, IL). Protein from K562 cells and staged zebrafish embryos were used for positive and experimental controls respectively.

Twenty-five ug of K562 cell protein and 75 ug of zebrafish protein at 18, 24, 32, and 36 hpf was loaded into NuSep 4-20% LongLife gels for electrophoresis at 50v for 30 min and 90v until completion (≈1 hour). Protein was then blotted onto Bio-Rad Immun-Blot PVDF membranes for 1 hr at 100v. Non-specific binding sites were blocked by incubation in blotto at room temperature for ≥ 5 hours; blotto contained 5 g of carnation non-fat powdered milk and 100 ml TBS with 0.2% triton. For experimental and positive controls, membranes were then incubated in 1:200 sc-131 primary antibody at 4°C overnight. Negative controls were incubated at 4°C overnight in sc-131 antibody pre-absorbed with sc-131 peptide (4:1 concentration of peptide: antibody). The following day membranes were washed in TBST; 3 x 15 min. TBST at a final pH of 7.4 contained 1.21 g/L tris base, 8.76 g/L NaCl, and 2 ml/L of triton. Following TBST washes, membranes were incubated in 1: 3000 goat-α-rabbit-AP antibody (Bio-Rad, Hercules, CA) for 1 hour, and stained by NBT/BCIP reaction. Membrane

images were procured using an Epson Stylus NX400 Series scanner and compiled for figures by using the program Microsoft PowerPoint 2008 for Mac.

Results

Sequencing of cDNA

After sequencing the cDNA clone (ID: 3857626, Accession: EB951650) that was listed as a mRNA sequence of 737 base pairs (bp) by OpenBiosystems, it was discovered that it was actually a 3893 bp clone containing a translatable region of 332 amino acids (aa). The remaining 2897 bp following the translatable region contained numerable stop codons. Our clone was incomplete at the 5' end but did contain and a poly-a tail at the 3' end. A protein BLAST analysis using the NCBI database identified two predicted *Danio rerio* v-Abl1 oncoprotein homologs: isoform1 (XP_001337829.1) and isoform2 (XP_001337899.1), which respectively are 1079 aa 1060 aa in length. These sequences had 99% identity when pairwise aligned with the translatable region of our cDNA clone. The 5' portion of the predicted *D. rerio* v-Abl1 homolog and our sequenced clone has been compiled to show a tentative full length *abl* mRNA sequence (see Figure 5). Base pairs 1-2290 represent the predicted sequence available online (XM_001337793.3). The following 996 bp (base pairs 2291-3287) region represents the translatable region of our clone and displays corresponding codons above. The blue underlined portion indicates the sequence transcribed during the generation of DIG-RNA probes; single underlined portions of both colors (blue and black) correspond to the areas we have sequenced. Colored boxes highlight the primers used for sequencing.

When the 332 aa translatable region was aligned with other annotated Abl1 sequences, we observe a pairwise alignment score of 51 to *H. sapiens* Abl1. However, when the full length predicted *D. rerio* v-Abl1 sequence (XP_001337899.1) is used, the pairwise alignment score increased to 71 when compared to *H. sapiens* Abl1. The deduced amino acid sequence was aligned with other known Abl1 sequences and the Bcr-Abl form of human origin (see Figure 6). A phylogenetic tree comparing the predicted *D. rerio* Abl (XP_001337899.1) and other Abl1 homologs was also constructed (see Figure 7).

Whole-mount *in situ* hybridization

I have examined expression of the *abl* gene using *in situ* hybridization at embryonic stages from the cleavage and blastula period to late pharyngula just prior to hatching. Embryos at the following stages were examined: 2, 12, 18, 24, 32, 36, and 48 hpf. There was no expression of the *abl* gene at 2 hpf; both positive and negative controls are absent of NBT/BCIP staining (see Figure 8A).

Expression begins to appear at 12 hpf during the bud stage and was observed in several regions of the developing neural plate: anteriorly in the deepest regions of the polster closest to the midsagittal furrow where prechordal plate hypoblast accumulates, within the posterior region of the neural plate at the site of early somite development, and within the tailbud (see Figure 8B-E). Expression is strongest in the polster with lighter staining seen in the posterior regions of the neural plate and tail bud. At 18 hpf, expression is concentrated at the polster (see Figure 9A-C). Ventral view shows that *abl* expression in concentrated in the deepest areas of the polster closest to the midsagittal furrow with minimal expression seen within the tailbud (see Figure 9C).

Expression is anteriorly localized at 24 hpf, (see Figure 9D,E). Expression is also seen through the midsection of the body strengthening mildly at the tail and PBI (see Figure 9D,F). A similar pattern is seen at 32 hpf with the strongest expression in the head and expression continuing through the midsection and into the tail and PBI (see Figure 9G-J). At 36 hpf, expression is concentrated in the head and dissipates abruptly where somite segmentation begins (see Figure 10A,C). Light expression is seen along regions of tail immediately above the notochord (see Figure 10A, B, D).

At 48 hpf, expression of *abl* is diffuse along the midline of the tail and midsection and splits immediately above the center of the yolk sac into a Y shaped pattern with expression in the head concentrating at regions between the developing eyes (see Figure 10G). Intense expression in the head corresponds to areas of the future eye, telencephalon and midbrain and within the endoderm deepest to the yolk sac (see Figure 10F). Expression of *abl* is not seen in negative controls using the sense RNA probe (see Figure 11).

Whole-mount immunohistochemistry

I have also examined protein expression of Abl using the SC-131 antibody specific for the kinase domain of human Abl1 at the following embryonic stages: 18, 24, and 32 hpf. At 18 hpf there is minimal protein expression concentrated in the tail bud (see Figure 12A). Stronger expression is seen within the PBI and caudal vein plexus at 24 hpf and 32 hpf (see Figure 12 C,E). There is intense staining at the tail tip and at a region anteriorly adjacent to the tail tip at 24 hpf (see Figure 12C). Negative controls were absent of any staining (see Figure 12B,D,F)

Western blot

A western blot with zebrafish embryonic protein at 18, 24, 32, and 36 hpf was conducted with the sc-131 antibody. A band of slightly >100 kD is present in lanes 1-4 corresponding to embryos at 18-36 hpf (see Figure 13A). Expression is greatest at earlier time stages and progressively diminishes in strength at later time stages. The molecular weight is congruous with the predicted molecular weight of *D. rerio* v-Abl1 (117 kD); therefore, it is likely that this band represents the Abl homolog. It is also evident that there are multiple bands present at molecular weights too small to be considered Abl protein. Figure 13B contains the addition of the K562 positive control in lane 1 with lanes 2-5 corresponding to embryos at 18-36 hpf. Lane 1 contains bands within the range 150-250 kD which is also in agreement with the known Bcr-Abl molecular weights of 190, 210, and 230 kD (Amar et al., 1992). However, this lane also contains other bands of incorrect weights. In a pre-absorption negative control (4:1 peptide: antibody concentration), all bands diminish in strength but are still present (see Figure 13C).

Discussion

Data at the DNA, RNA, and protein level obtained in this research allow several conclusions to be made concerning the existence of an Abl homolog in zebrafish. Sequencing of a *D. rerio* cDNA clone, translation by ExPASy, and subsequent protein blast searches return *abl* homologs in humans, mice, and a variety of other organisms. A predicted *D. rerio* Abl protein 99% identical to our clone has 71% identity to Abl1 of human origin indicating homology. The predicted *D. rerio v-Abl1* and *v-Abl2* isoforms, which are publicly available on the NCBI database, contain a C-terminus with F-Actin and G-Actin binding sites, the Kinase domain, and the SH2 domain. Due to the high similarity of zebrafish DNA sequences and the presence of conserved domains, these results suggest that the zebrafish Abl protein could have similar cytoskeletal functions based on its C-terminus binding sites. In addition to sequence analysis, RNA investigations validate the possibility of an Abl homolog in zebrafish.

The segmentation period in zebrafish is a key time when the brain rudiment is being sculptured (Kimmel et al., 1995)**.** Prior to this segmentation period, during the 64-cell stage at 2 hpf we observed an absence of *abl* gene expression. However, beginning at 12 hpf, *abl* gene expression was seen anteriorly in the deepest regions of the polster closest to the midsagittal furrow where the prechordal plate thickens (Kimmel et al., 1995). This thickening region of the neural plate occurs at the animal pole and is caused by the accumulation of prechordal plate hypoblast; it represents the site of future brain and eye

development. Expression of the *abl* gene was present here within the midsagittal furrow from 12-48 hpf. This furrow, caused by the formation of brain rudiment, contained *abl* expression linking the gene with neural plate formation and morphogenesis of the neural rod (see Figure 9C) (Kimmel et al., 1995) indicating that it is active during these time stages.

In the brain of adult mice, Abl2 is found in high amounts and co-localizes with Abl1 during neurulation, indicating the involvement of Abl in embryonic neurogenesis (Koleske et al., 1998). Studies in *Drosophila* and *Mus musculus* have demonstrated the importance of the *Abl* gene in axon guidance and synapse formation in the developing central nervous system (Lin et al., 2009; Stevens et al., 2008). These proteins are also highly active in retinal cells of *Drosophila* (Henkemeyer et al., 1990). Our zebrafish embryos showed strong expression in the eye region from 24-48 hpf and within sites corresponding to development of brain tissue. Our results, in accordance with the literature suggest that *abl* has a function in the development of the central nervous system and eyes of the embryonic zebrafish from 12-48 hpf.

Another key avenue of investigation is the involvement of *abl* in hematopoiesis. Its function in zebrafish hematopoiesis can be examined by observing two regions: the AGM and PBI. Both regions are known to harbor hematopoietic progenitor cells beginning at 24 hpf and peaking at 30 hpf. In zebrafish, HSCs are present in the AGM from 28-48 hpf and contain several genes involved in hematopoiesis (Bertrand et al., 2007); the gene and protein expression patterns of abl that we have observed are similar to patterns discussed in the literature. Within the tail, we see strongest expression at 24 and 32 hpf and a decrease in tail expression of abl at 36 hpf. In addition, presence of *abl* transcripts and peptides in the PBI was strongest at 24-32 hours (see Figure 9F,I) linking *abl* to the emergence or migration of

HSCs in the AGM. Occurring around 22 hpf, studies also show that myeloid cells group in the rostral region of the embryo and are scattered around the margins adjacent to the yolk sac. Embryos at 24 hpf showed staining clustered around the yolk sac but it is undetermined whether this staining represents myeloid cell grouping (see Figure 9). Expression at these sites adjacent to the yolk sac may represent *abl* function in hematopoiesis or neurulation. It is possible that regions in the head represent neurulation functions and regions closer to the sinous venosus and mid section represent myeloid cell clustering.

Transcripts of *abl* were found along the midline of the body above the yolk sac extension and the tail at 48hpf. This expression could represent *abl* presence in the dorsal aorta, a site of HSC emergence. The gene may be involved in the development of HSCs at this region. Expression of the gene split into a Y shape displaying lateral arms pointing towards the head when dorsally viewed; this split in the expression pattern is consistent with the splitting of the dorsal aorta into the lateral dorsal aortas at the sinus venosus of the heart. After branching, the lateral dorsal aortas supply the primitive internal carotid artery which line the inner margins of the developing eye (Isogai et al., 2001); *abl* may be involved with vascular formation of these vessels. However, immediately above these two vessels lie the primordial hindbrain channel and the primordial midbrain channel (Isogai et al., 2001). Expression within these veins would block the view of the underlining lateral dorsal aortas so it is unclear if *abl* is expressed in these vessels or the deeper lateral dorsal aortas.

Protein studies are consistent with RNA expression in the PBI at 24 hpf and 32 hpf. Both ISH and IHC identify abl expression within this region immediately posterior to the yolk sac extension at times correlating to emergence of the EMP and production of erythrocytes and monocytes. However, expression of the abl protein within the head regions

does not match our previously described localization of *abl* gene expression. In western blot studies, pre-absorption of the primary antibody with peptide did not completely compete out bands of correct molecular weight (see Figure 13C). All bands, of correct or incorrect weight, were partially competed out indicating two possible situations: the primary antibody was pre-absorbed with an inadequate concentration of peptide, or that the primary antibody is not highly specific to the abl1 protein. Future protein studies will require the use of a monoclonal antibody and peptide to produce definitive results.

Through the sequencing of the zebrafish genome, we can now examine specific sequence identities shared with humans. There was a highly identical sequence within the fish and we have potentially identified it as an Abl ortholog. We examined this ortholog on several levels by cDNA clone sequencing, RNA *in situ* hybridization, and protein immunohistochemistry. This multifaceted investigation revealed the presence of abl in sites of central nervous system development and early definitive hematopoiesis at corresponding time points. Temporal and spatial expression indicates that the abl protein is expressed within the PBI during the emergence of the erythromyeloid progenitor and other HSCs. Based on these results it is probable that the abl tyrosine kinase in zebrafish has multiple cellular functions in the early morphogenesis of the fish. In other species, Abl serves multiple functions during embryonic development and specific roles later (Sirvent et al., 2008). Finally, many of Abl's known molecular partners have been identified and examined in zebrafish: p73, p53, HS1 and the src kinase family are all active in the fish indicating the possibility of abl kinase actions in zebrafish regulatory networks.

Our investigations of the Abl gene and protein in combination with the existing literature support the existence of conserved hematopoietic and neurogenic functions of Abl

in zebrafish. This protein, if mutated to produce a Bcr-Abl isoform, could become oncogenic providing possible direction for further research of the Abelson tyrosine kinase's molecular activity in zebrafish. Future studies to definitively establish Abl homology in zebrafish would entail the use of a monoclonal antibody for IHC and western blots. This antibody would be expected to completely compete out protein bands with correct molecular weight. Additionally, it would be pertinent to examine gene and protein expression at later stages in development and conduct tissue sectioning to more effectively establish localization. Several studies could be conducted to examine the functionality of the abl gene and protein in zebrafish: link abl to a green fluorescent protein to examine *in vivo* expression, knockdown abl expression to address how essential it is in early development, and co-localize abl with genes and proteins of known function in zebrafish.

Table 1. Primers used for cDNA clone sequencing. Primers were designed with MacVector and ordered through Eurofins MWG Operon. Sequencing reactions involving the *Danio rerio* cDNA clone (ID: 3857626) were performed by Cornell Life Sciences Core Laboratories Center and Mount Desert Island Biological Station.

Primer Name	Nucleotide Sequence
5A	5'-TCTGGAAAGACCTCAAGGAG-3'
5B	5'-TCCGCAGGACTTCTCAAAGC-3'
5C	5'-CCATTTGCCGTTTCACAC-3'
3A	5'-CTACACCAAAAACCACATCG-3'
3B	5'-GCAAATGGTGCTTTAGGC-3'

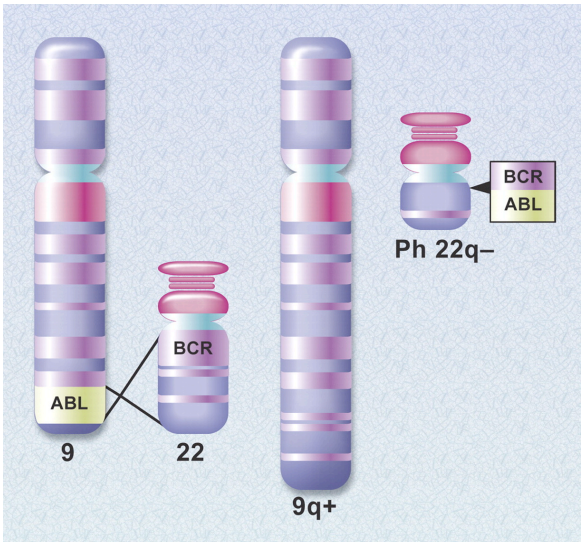

(Druker, 2008)

Figure 1. The Philadelphia chromosome. The *Abl* gene originating on the long arm of chromosome 9 becomes translocated onto the long arm of chromosome 22 at the break point cluster region (*Bcr* gene). This creates a shortened chromosome 22, the *Bcr-Abl* fusion gene, and a lengthened chromosome 9. A portion of the *Bcr* gene is also translocated to chromosome 9 (Druker, 2008).

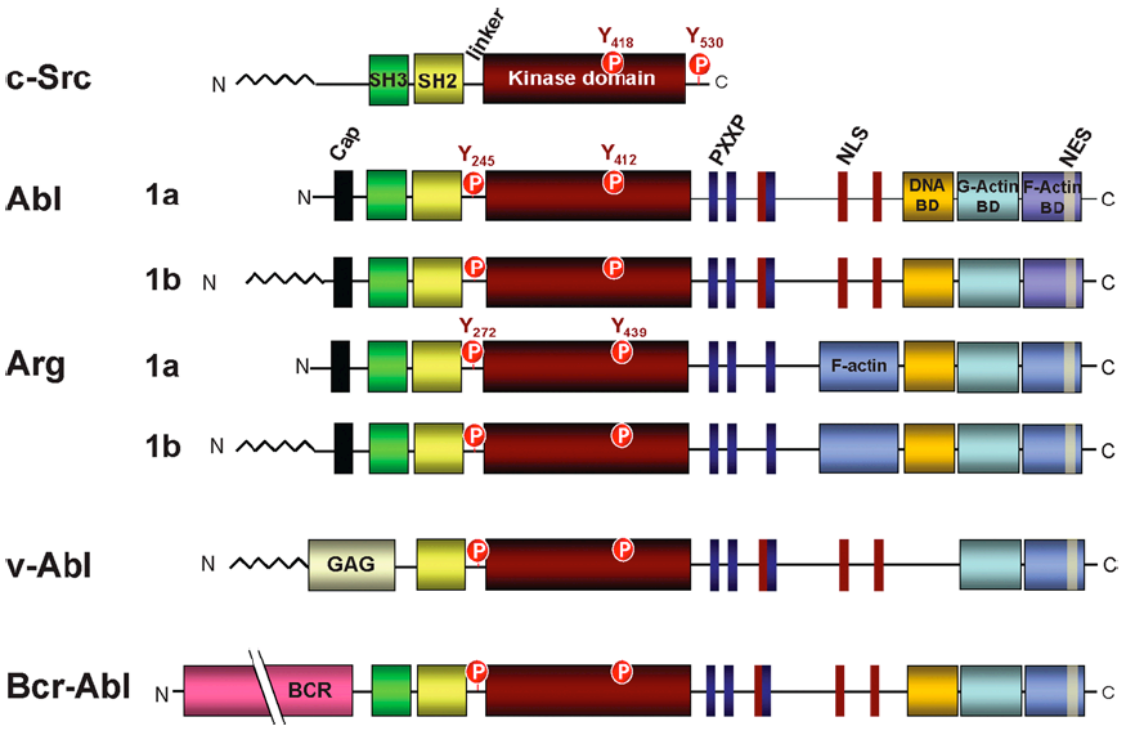

(Sirvent et al., 2008)

Figure 2. Isoforms of the Abelson protein. A variable N-terminus is followed by a Cap (certain isoforms), the SH3, SH2, and Kinase domains. In addition, a PXXP (proline rich sequences), a NLS (nuclear localization signals), a DNA binding domain, a G-Actin, and a F-Actin binding domain are found in some isoforms. The mutated Bcr-Abl isoform and the v-Abl isoform contain the addition of the BCR and GAG domains, respectively. This results in the loss of the variable N-terminus. Phosphorylation sites resulting in Abl activation are indicated by red circles (Sirvent et al., 2008).

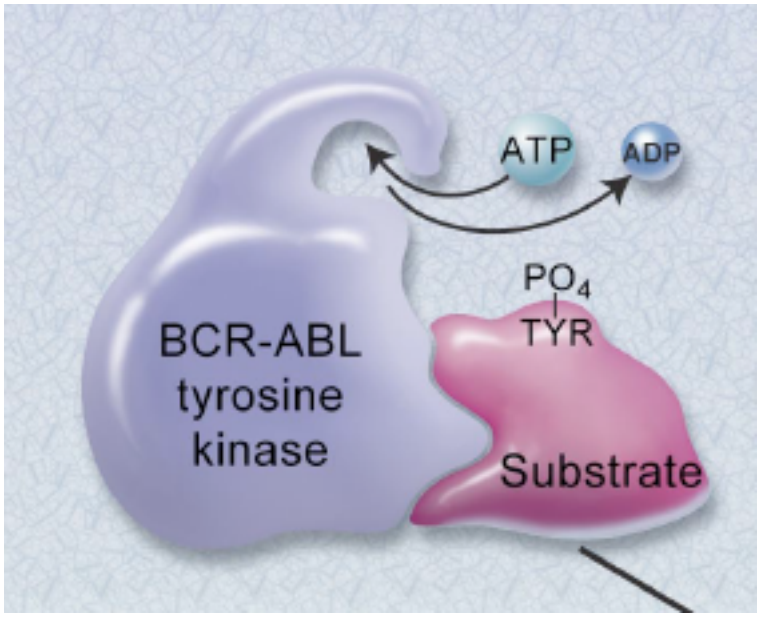

(Druker, 2008)

Figure 3. The molecular activity of the Bcr-Abl tyrosine kinase. When the tyrosine kinase and substrate protein are properly bound, a phosphate group (PO_4) from ATP is transferred to a tyrosine (TYR) residue on the substrate protein producing ADP and substrate protein activation. This action is completed in the same molecular manner within all Abl isoforms, but with varying strengths (Druker, 2008).

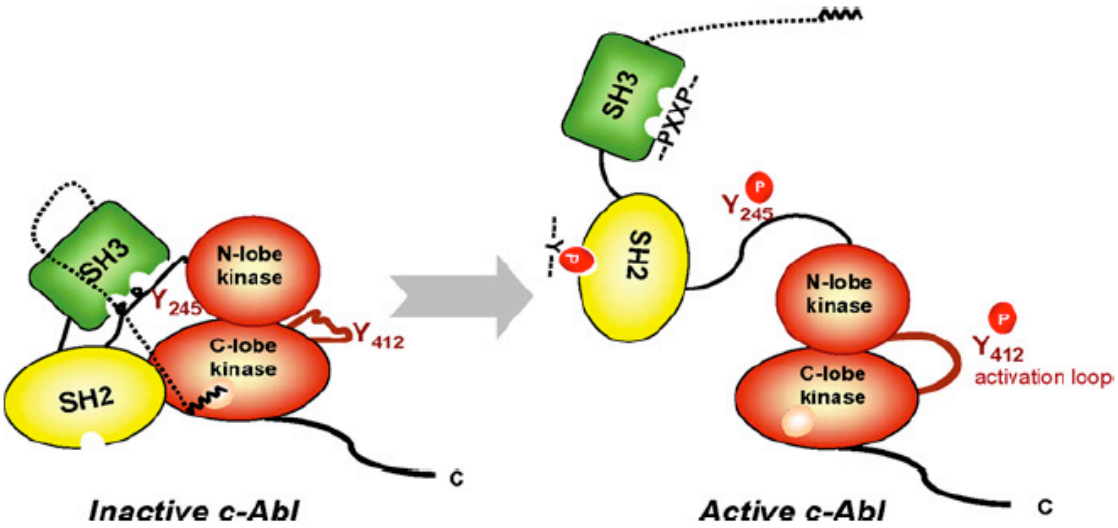

(Sirvent et al., 2008)

Figure 4. Inactive and active conformations of c-Abl. The binding of the N-terminal end with a pocket on the C-lobe kinase, SH2 to the C-lobe of the Kinase domain, and SH3 to the linker region keeps Abl in a closed shape. Phosphorylation at the SH2 domain, Y245, Y412, or loss of the N-terminus causes Abl to assume an open conformation and become activated (Sirvent et al., 2008).

```
1          atggggcagc
11         agccaggaaagttagtgggtgagcagaggagaccgagcctgccggcactgcccttcatca
71         aggccgcggggaggagagagacgccccggcacggagcaccgcactgcaatgtgttcacgg
131        tccacgagtctcggccggatttcgatccccccggtctttcagaagcggcgcgctggaact
191        ctaaagagaacctgctgtcgggacccagcgaaaatgaccccaatctgttcgtggcgctgt
251        acgactttgtggcgagcggcgacaacactctcagcataactaaaggagagaagctgaggg
311        ttctgggatacaatcacaatggtgagtggtgcgaggcgcagaccaagaacgggcagggct
371        gggtgcccagcaactacatcacgcccgtcaacagcctggagaagcacagctggtaccacg
431        ggccggtgtccagaaatgctgcagagtacctgctgagcagcggcatcaacggcagcttcc
491        tggtgcgggagagcgagagcagcccgggacagcgctccatatcactgcgctacgagggac
551        gagtctaccactaccgcattaatacagcctcagacggcaagctgtacgtgtcgtccgaga
611        gccgctttaacactctagcagagctggttcatcatcactccacggtctctgacggtctga
671        tcaccacgctgcattaccccgcacccaaacgcaacaaacccaccatctacggcgtctctc
731        caaactacgacaagtgggagatggagcgcacggacatcaccatgaagcacaagctgggcg
791        gagggcagtacggggaggtgtacgagggcgtgtggaagaagtacagcctcaccgtggcgg
851        tgaaaacactgaaggaagacaccatggaagtggaggagtttctgaaagaagctgcagtga
911        tgaaagaaatcaaacacccaaacctggtgcagctcttaggcgtctgcactcgggaacctc
971        cgttctacatcatcactgagttcatgacacatggaaacctgctggattacctgcgcgagt
1031       gtaaccggcaggaggtgaacgctgtggtgctgctctacatggccacgcagatctcctccg
1091       ccatggagtacctggagaagaagaacttcatccacagggatctggcagcccgtaactgct
1151       tggtcggggaaaacaacctggttaaagtggcagattttgggctaagccggctgatgacgg
1211       gagacacatacacagcccacgctggagcaaagttccccattaaatggactgcgccggaga
1271       gtctggcctataacaagttctccatcaagtcagacgtgtgggcatttggagtcctgcttt
1331       gggagatcgccacctatgggatgtctccgtatccaggaatcgacctgtctcaggtgtatg
1391       agctgctggagaaagactaccgcatggacagacccgagggatgcccagagaaagtctatg
1451       agctcatgagggcctgttggaggtggaaccctgccgagcgcccttcttttgctgagaccc
1511       atcaggcgttcgagaccatgtttcaagagtccagtatctctgatgaggtggagaaagagt
1571       tggggaaaaaaggaaagaagctgaccctgggaccaatacagcaggcgccagaacttccaa
1631       ctaaaaccaggacactacgaagacctacagacggcagggatggggacagtcccgccgagg
1691       ccgaggtcactggacccccgatgatgccgaggccactcctagatagcaacctgaatgaag
1751       ccagtctaaagataataaggataaatttcgaatgaatcccttcagttatattaagaaaaa
1811       gaagaggacggctccggcgccccccaaagcgcagcagctcctttgggaagatggacggaca
1871       cctagaccgtagaggattgggtactgactgcagggaggatttcagcaacgggtcttccac
1931       caatgatgccttaaacagcattgacccttgcaaattagttgggtcaaacagtaccacgac
1991       catcggggtcaccaacggagctccagtgtatcccggtcagctcttcccatctcatccacg
2051       gaaaaagggcactacatcgggtggtggagggaagcttgccacgactccacctccagagga
2111       ggactccatgtcaaactccaaacgcttcctacgatcttcttcttcctccagcatgcctcc
2171       aggctctgatcgcttcgaatggaagtccgtaaccctgccgcgggacattcagtcaacaca
2231       ccacgcgtccgcacattcagaggcaagccagttttacctcgtaagagctgcatgccacga
             P  R  V  R  T  F  R  G  K  P  V  L  P  R  K  S  C  M  P  R
2291       ggtggcacgcttaccccaccaccacgccttcccaagaaaagtgaagatgtttcagacgaa
             G  G  T  L  T  P  P  P  R  L  P  K  K  S  E  D  V  S  D  E
2351       gtcttcaaggactctgagtctagtcctggatcaagtcctttaactctgactcccaagcta
             V  F  K  D  S  E  S  S  P  G  S  S  P  L  T  L  T  P  K  L
2411       ggccgccgaccccaaacagaaagctccaaaactagtgccttacaaacagaggtattaaaa
             G  R  R  P  Q  T  E  S  S  K  T  S  A  L  Q  T  E  V  L  K
2471       cccaatgtgcttccacctcttggagacgaaggcagacctcgaagactcaaactgtcctct
             P  N  V  L  P  P  L  G  D  E  G  R  P  R  R  L  K  L  S  S
2531       gaaatcccaggacagagagagcgggagaaggggaagtttgcgaaacccaaacccgctccc
             E  I  P  G  Q  R  E  R  E  K  G  K  F  A  K  P  K  P  A  P
2591       cctcctcctccggtgtccagtgccaaatctggaaagacctcaaggagtccgacttttgag
             P  P  P  P  V  S  S  A  K  S  G  K  T  S  R  S  P  T  F  E
2651       gtgtcttcagataccaaagtcaagagttcactagactccgcagatcaaggcaaggctagt
             V  S  S  D  T  K  V  K  S  S  L  D  S  A  D  Q  G  K  A  S
2711       ctatcccaagaaagtgctaaaaagttgcccaaaaatggctcaaaggtaaacccctcgaag
             L  S  Q  E  S  A  K  K  L  P  K  N  G  S  K  V  N  P  S  K
2771       gcaggtgcgactgctcctctacctggaatgggagccagtcctgtggtcggggatccggga
```

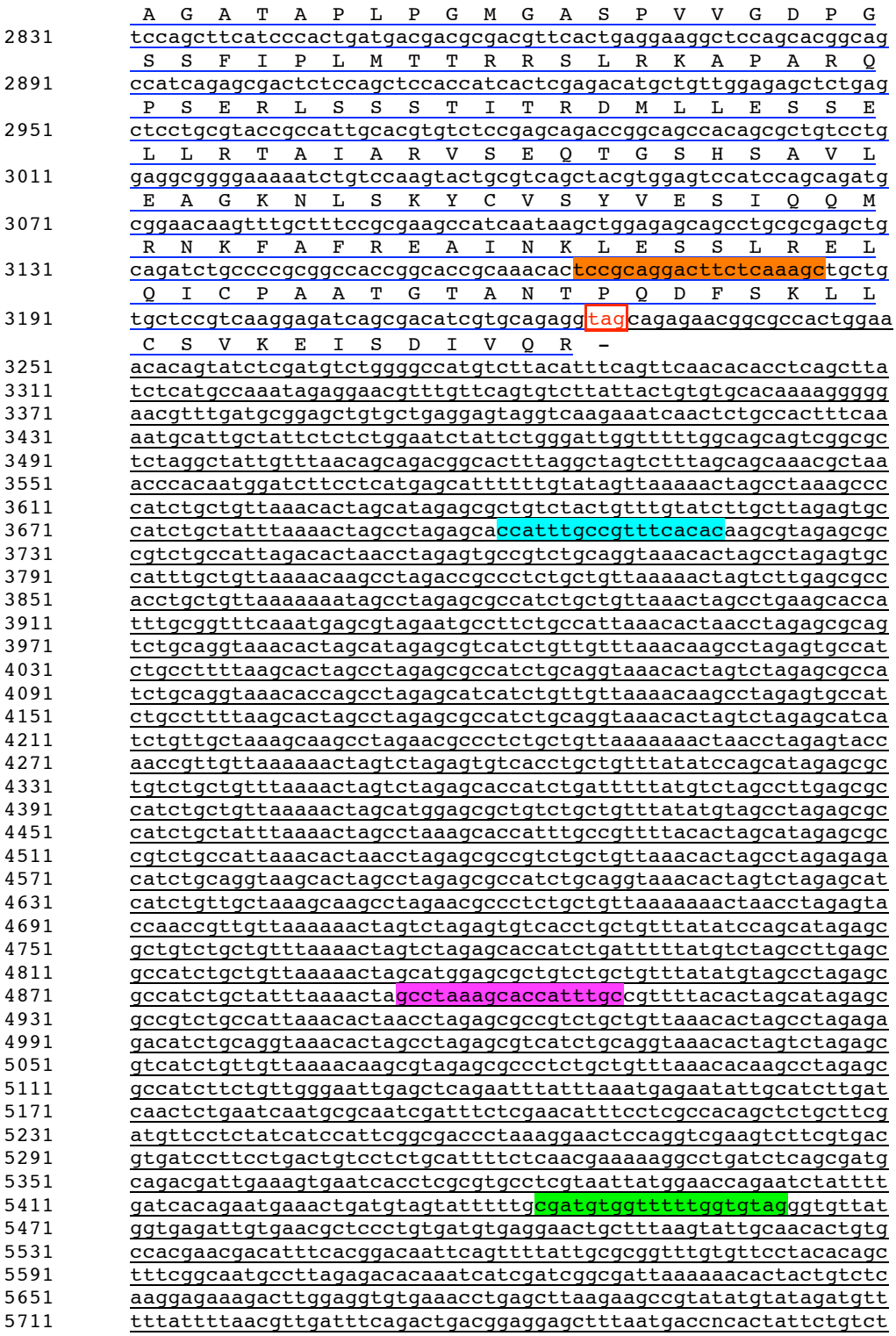
A G A T A P L P G M G A S P V V G D P G
2831 tccagcttcatcccactgatgacgacgcgacgttcactgaggaaggctccagcacggcag
S S F I P L M T T R R S L R K A P A R Q
2891 ccatcagagcgactctccagctccaccatcactcgagacatgctgttggagagctctgag
P S E R L S S S T I T R D M L L E S S E
2951 ctcctgcgtaccgccattgcacgtgtctccgagcagaccggcagccacagcgctgtcctg
L L R T A I A R V S E Q T G S H S A V L
3011 gaggcggggaaaaatctgtccaagtactgcgtcagctacgtggagtccatccagcagatg
E A G K N L S K Y C V S Y V E S I Q Q M
3071 cggaacaagtttgctttccgcgaagccatcaataagctggagagcagcctgcgcgagctg
R N K F A F R E A I N K L E S S L R E L
3131 cagatctgccccgcggccaccggcaccgcaaacactccgcaggacttctcaaagctgctg
Q I C P A A T G T A N T P Q D F S K L L
3191 tgctccgtcaaggagatcagcgacatcgtgcagaggtagcagagaacggcgccactggaa
C S V K E I S D I V Q R -
3251 acacagtatctcgatgtctggggccatgtcttacatttcagttcaacacacctcagctta
3311 tctcatgccaaatagaggaacgtttgttcagtgtcttattactgtgtgcacaaaaggggg
3371 aacgtttgatgcggagctgtgctgaggagtaggtcaagaaatcaactctgccactttcaa
3431 aatgcattgctattctctctggaatctattctgggattggtttttggcagcagtcggcgc
3491 tctaggctattgtttaacagcagacggcactttaggctagtctttagcagcaaacgctaa
3551 acccacaatggatcttcctcatgagcatttttttgtatagttaaaaactagcctaaagccc
3611 catctgctgttaaacactagcatagagcgctgtctactgtttgtatcttgcttagagtgc
3671 catctgctatttaaaactagcctagagcaccatttgccgtttcacacaagcgtagagcgc
3731 cgtctgccattagacactaacctagagtgccgtctgcaggtaaacactagcctagagtgc
3791 catttgctgttaaaacaagcctagaccgccctctgctgttaaaaactagtcttgagcgcc
3851 acctgctgttaaaaaaatagcctagagcgccatctgctgttaaactagcctgaagcacca
3911 tttgcggtttcaaatgagcgtagaatgccttctgccattaaacactaacctagagcgcag
3971 tctgcaggtaaacactagcatagagcgtcatctgttgtttaaacaagcctagagtgccat
4031 ctgccttttaagcactagcctagagcgccatctgcaggtaaacactagtctagagcgcca
4091 tctgcaggtaaacaccagcctagagcatcatctgttgttaaaacaagcctagagtgccat
4151 ctgccttttaagcactagcctagagcgccatctgcaggtaaacactagtctagagcatca
4211 tctgttgctaaagcaagcctagaacgccctctgctgttaaaaaaactaacctagagtacc
4271 aaccgttgttaaaaaactagtctagagtgtcacctgctgtttatatccagcatagagcgc
4331 tgtctgctgtttaaaactagtctagagcaccatctgatttttatgtctagccttgagcgc
4391 catctgctgttaaaaactagcatggagcgctgtctgctgtttatatgtagcctagagcgc
4451 catctgctatttaaaactagcctaaagcaccatttgccgttttacactagcatagagcgc
4511 cgtctgccattaaacactaacctagagcgccgtctgctgttaaacactagcctagagaga
4571 catctgcaggtaagcactagcctagagcgccatctgcaggtaaacactagtctagagcat
4631 catctgttgctaaagcaagcctagaacgccctctgctgttaaaaaaactaacctagagta
4691 ccaaccgttgttaaaaaactagtctagagtgtcacctgctgtttatatccagcatagagc
4751 gctgtctgctgtttaaaactagtctagagcaccatctgatttttatgtctagccttgagc
4811 gccatctgctgttaaaaactagcatggagcgctgtctgctgtttatatgtagcctagagc
4871 gccatctgctatttaaaactagcctaaagcaccatttgccgttttacactagcatagagc
4931 gccgtctgccattaaacactaacctagagcgccgtctgctgttaaacactagcctagaga
4991 gacatctgcaggtaaacactagcctagagcgtcatctgcaggtaaacactagtctagagc
5051 gtcatctgttgttaaaacaagcgtagagcgccctctgctgtttaaacacaagcctagagc
5111 gccatcttctgttgggaattgagctcagaatttatttaaatgagaatattgcatcttgat
5171 caactctgaatcaatgcgcaatcgatttctcgaacatttcctcgccacagctctgcttcg
5231 atgttcctctatcatccattcggcgaccctaaaggaactccaggtcgaagtcttcgtgac
5291 gtgatccttcctgactgtcctctgcattttctcaacgaaaaaggcctgatctcagcgatg
5351 cagacgattgaaagtgaatcacctcgcgtgcctcgtaattatggaaccagaatctatttt
5411 gatcacagaatgaaactgatgtagtatttttgcgatgtggtttttggtgtaggtgttat
5471 ggtgagattgtgaacgctccctgtgatgtgaggaactgctttaagtattgcaacactgtg
5531 ccacgaacgacatttcacggacaattcagttttattgcgcggtttgtgttcctacacagc
5591 tttcggcaatgccttagagacacaaatcatcgatcggcgattaaaaaacactactgtctc
5651 aaggagaaagacttggaggtgtgaaacctgagcttaagaagccgtatatgtatagatgtt
5711 tttattttaacgttgatttcagactgacggaggagctttaatgaccncactattctgtct

```
5771    taaccagtcttttctcgttgttttgctcgtttagttaaaataatgcccttgttttcagta
5831    ttagtttgtattttccaacactttgccgtcagactgcgatgcctgaggaggaccncacgc
5891    tgccttgatttcaacacgccaccagtgttgctgacgtttttatatcttgtcctttagaga
5951    tcatgccactacttttacatttgtattcaagcctcacttttttttaatgctcgtttctgta
6011    aatacacacttgttttctcctatcggttgattcttcttgtaaccctggtgcaatgtgtgt
6071    tgcatacaatacagttttgctacttgaacgaaaaaaaaaaaaaaaaaaaaaaa
```

Figure 5. Nucleotide and deduced amino acid sequence of the putative *Danio rerio* Abelson 1 homolog. Underlined regions indicate regions we have sequenced from *D. rerio* cDNA (clone ID: 3857626); other regions were obtained from predicted Abl1 homolog on NCBI (XM_001337793.3). Blue underlined region indicates translatable region of our clone used in protein blasts. Capital letters above nucleotide sequence in the translatable region indicate the amino acid sequence. Colored regions indicate site of primers for sequencing reactions. Red box and text indicates start and stop codons.

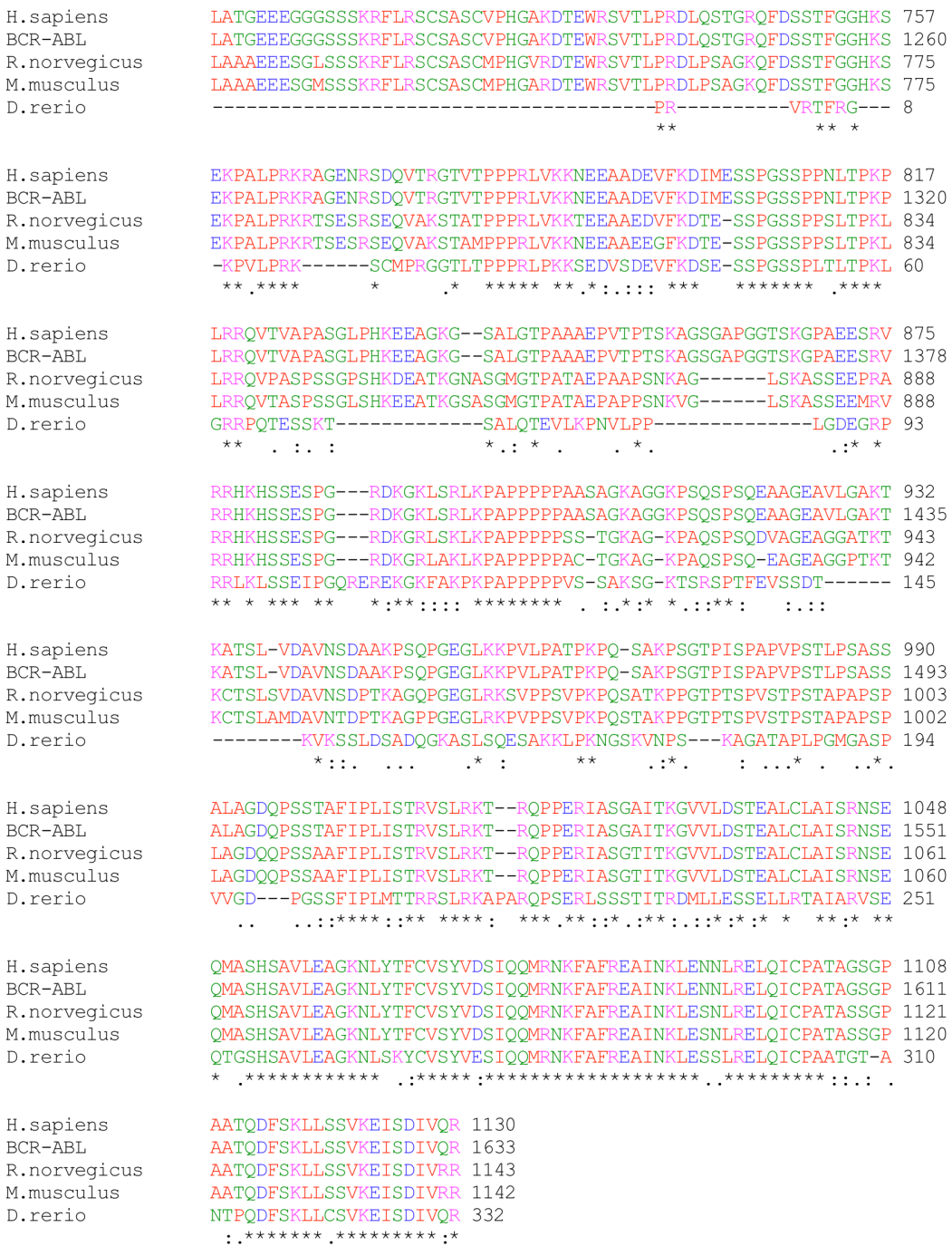

Figure 6. Amino acid sequence alignments of Abl1 orthologs and Bcr-Abl. All sequences were obtained through the NCBI database: *Danio rerio* (cloneID:3857626), *Homo sapiens* (NP_005148.2), *Mus musculus* (NP_001106174.1), *Rattus norvegicus* (ABC46642.1), Bcr-

Abl fusion kinase (ABX82702.1). Alignment corresponds to translatable region of the *D. rerio* clone. Alignment was generated using ClustalW2 with the following settings: gap opening penalty = 10, gap extension penalty =0.2, protein matrix = Gonnet. Amino acids colors indicate basic properties: RED = small + hydrophobic, BLUE = acidic, MAGENTA = basic, GREEN = hydroxyl + amine + basic-Q. " ⋆ " indicates complete conservation and " : " indicates partial conservation of amino acid.

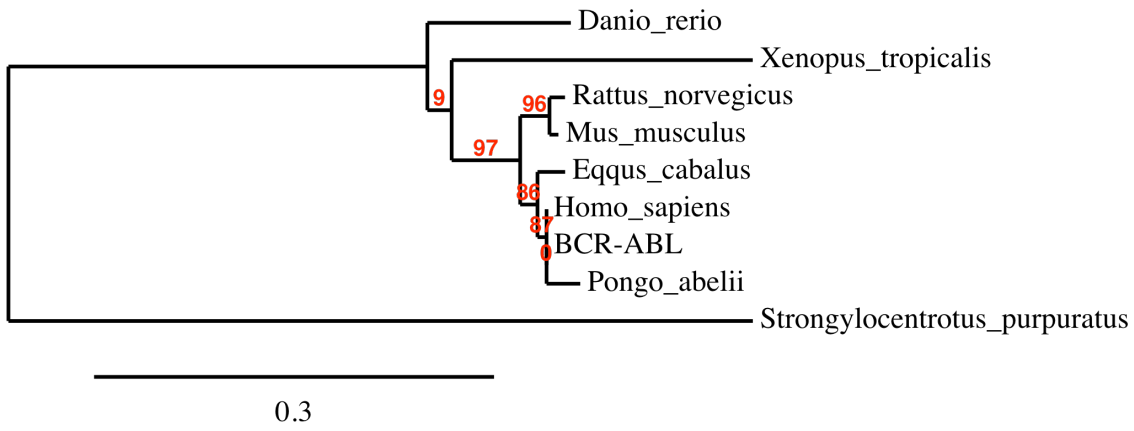

Figure 7. Phylogenetic tree of Abl orthologs and Bcr-Abl. Tree was constructed using Phylogeny.fr (http://www.phylogeny.fr/) using MUSCLE 3.7 for multiple sequence alignment, GBlocks 0.91b for alignment refinement, PhyML 3.0 aLRT for phylogeny, and TreeDyn 198.3 for tree rendering (Dereeper et al., 2008). Branch numbers represent percentage of clades grouped following 500 replications. Several species and the Bcr-Abl fusion kinase were examined: *Danio rerio* (XP_001337899.1), *Homo sapiens* (NP_005148.2), *Mus musculus* (NP_001106174.1), *Rattus norvegicus* (ABC46642.1), Bcr-Abl fusion kinase (ABX82702.1), *Pongo abelii* (XP_002833232.1), *Equus caballus* (XP_001917300.1), *Xenopus (Silurana) tropicalis* (XP_002936228.1), *Strongylocentrotus purpuratus* (XP_001203875.1).

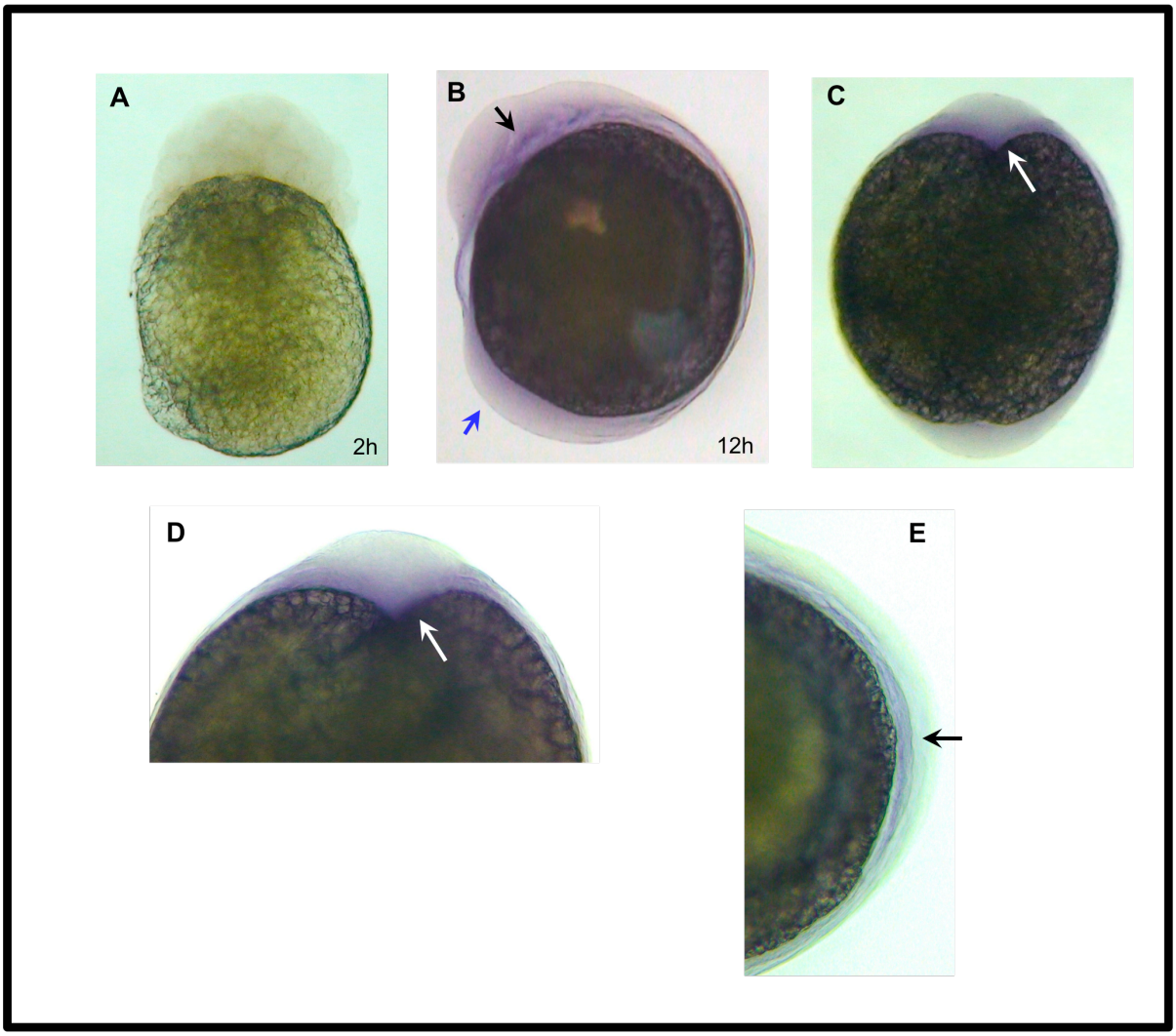

Figure 8. Whole-mount *in situ* hybridization of *abl* expression at 2 and 12 hpf. (A) 2 hpf, (B) 12 hpf embryo with polster indicated by black arrow, tailbud indicated by blue arrow, (C) ventral view at 12 hpf with midsagittal furrow indicated by black arrow, (D) 12 hpf magnification of polster from ventral view, (E) Posterior section of the neural plate at 12 hpf.

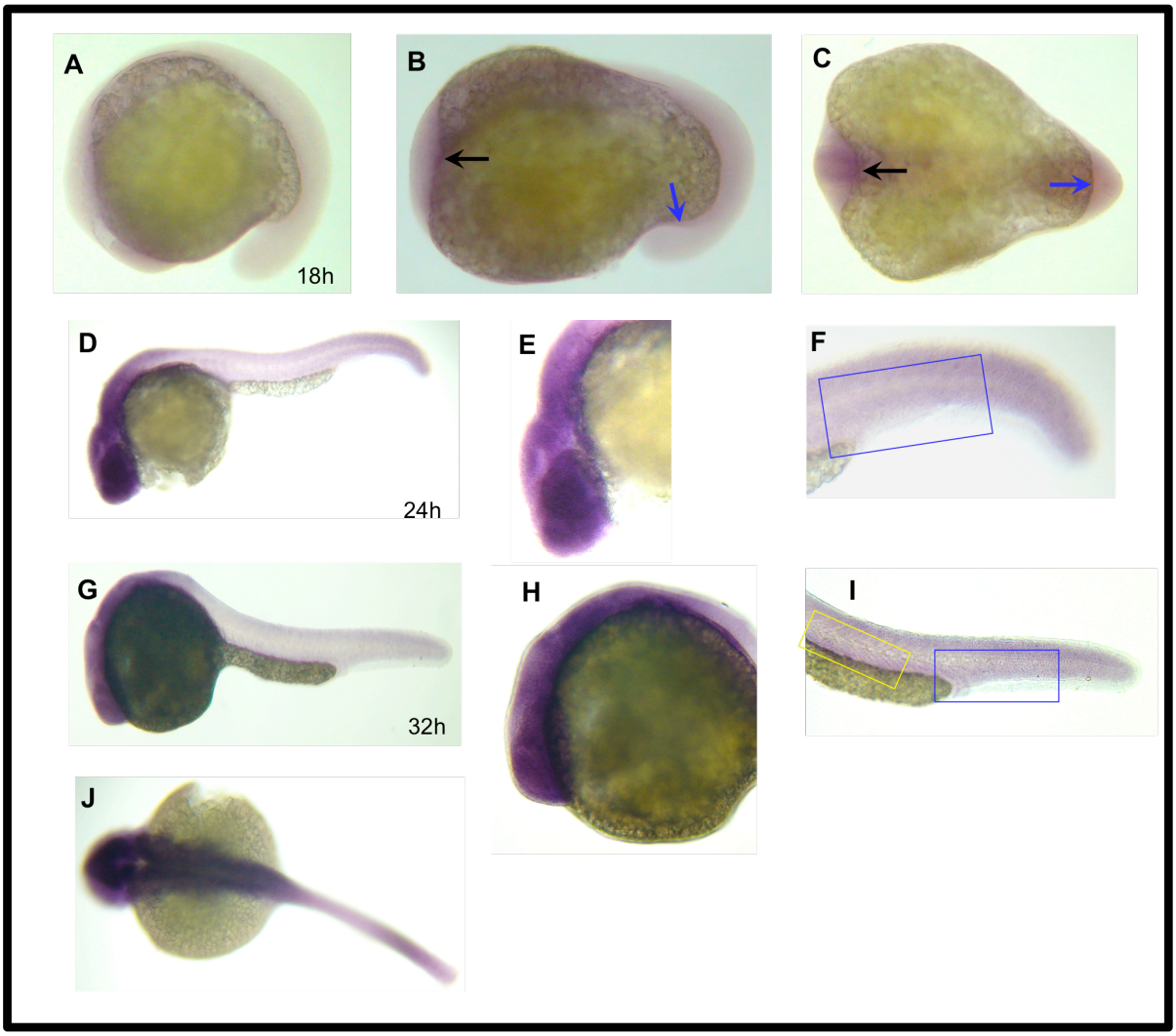

Figure 9. Whole-mount *in situ* hybridization of *abl* expression from 18-32 hpf. (A) 18 hpf showing expression along the midsagittal furrow, (B) 18 hpf embryo rotated to expose dorsal section of midsaggital line, black arrow indicates polster, blue arrow indicates tailbud, (C) 18 hpf ventral view showing expression at the midsagittal furrow, black arrow indicates polster, blue arrow indicates tailbud, (D) 24 hpf showing strong expression in the head and tail bud, (E) 24 hpf magnification of head at, (F) 24 hpf magnification of tail, blue box highlights PBI region, (G) 32 hpf showing strong expression in the head dissipating towards posterior sections, (H) 32 hpf magnification of the head showing strong expression, (I) 32 hpf magnification of the tail, blue box highlights PBI, yellow box highlights AGM region, (J) 32 hpf dorsal view.

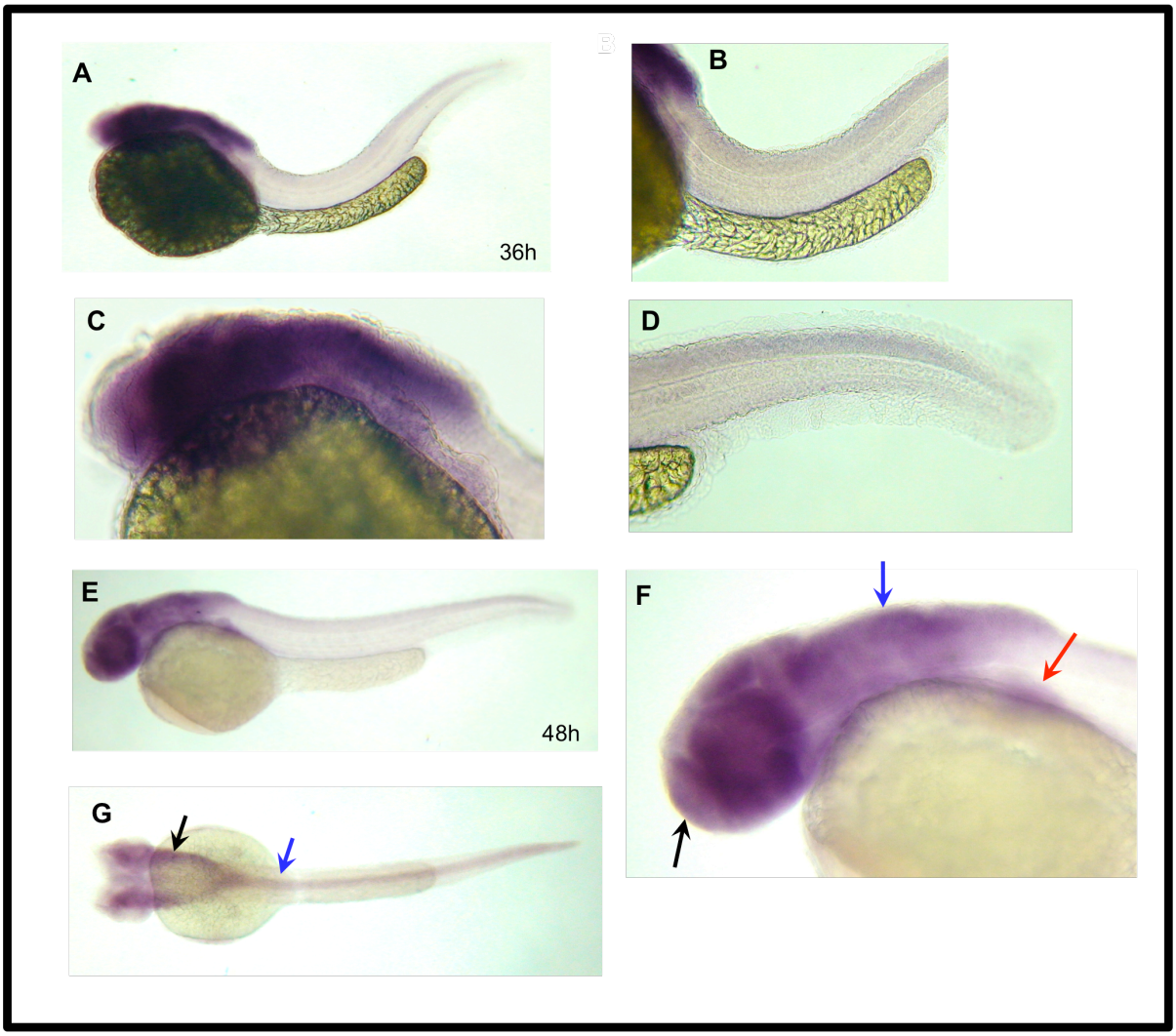

Figure 10. Whole-mount *in situ* hybridization of *abl* expression at 36 and 48hpf. (A) 36 hpf embryo with anterior to the left. Expression is strongest anteriorly but some expression is observed in the midsection and tail, (B) 36 hpf mid section and yolk sac extension magnification, (C) 32 hpf magnification of the head, (D) 36 hpf embryo showing magnification of PBI, (E) 48 hpf embryo showing strong expression anteriorly and weaker expression in the rest of the body, (F) 48 hpf embryo showing magnification of the head, black arrow indicates telencephalon, blue arrow indicates myelencephalon, red arrow indicates endoderm, (G) 48 hpf embryo at dorsal view showing expression along the midline, possible lateral dorsal aorta indicated by black arrow, possible dorsal aorta or notochord indicated by blue arrow, expression is also seen in the optic regions.

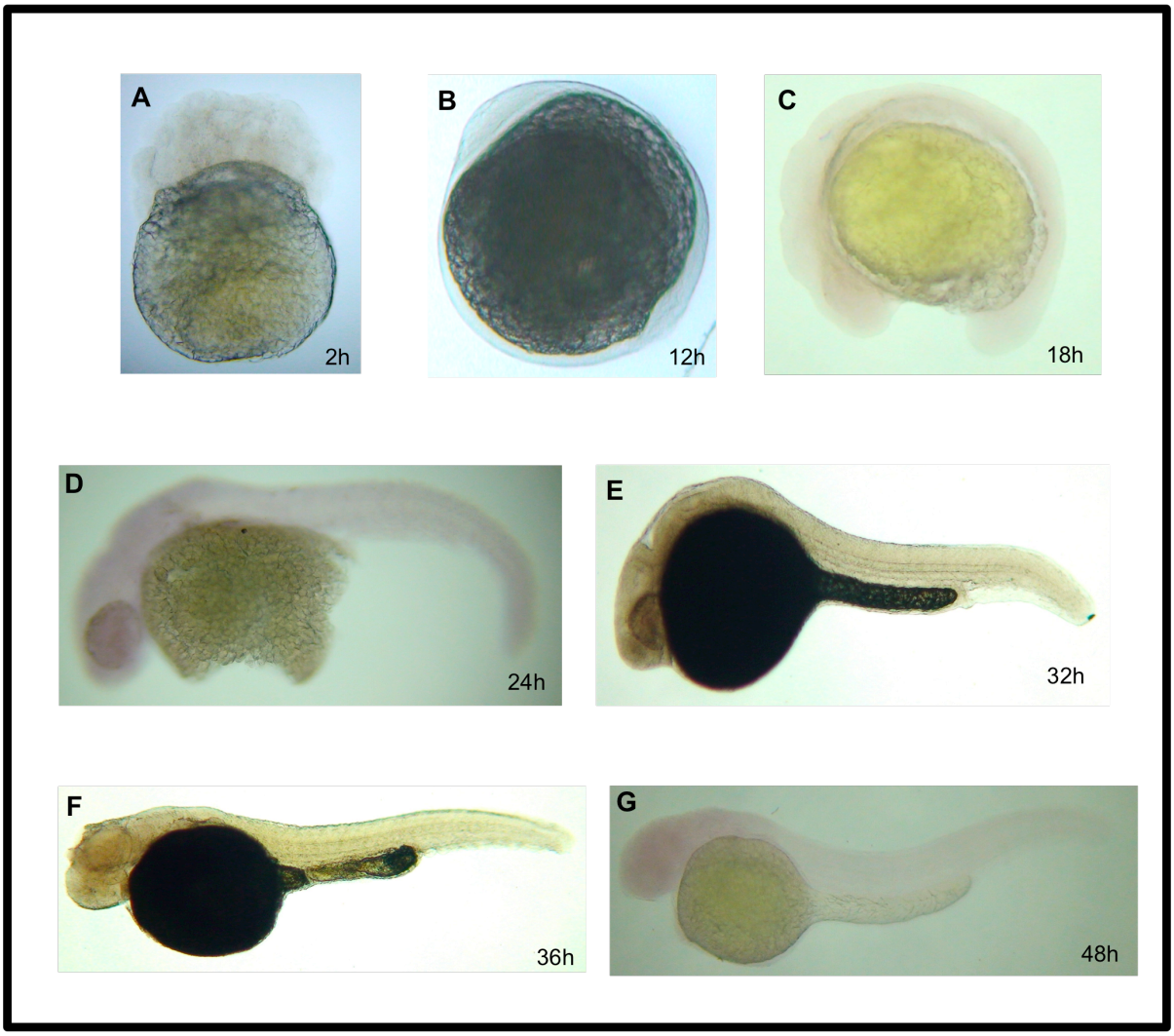

Figure 11. Whole-mount *in situ* hybridization negative controls. Hybridization reactions were performed with sense (negative control) probes from cleavage period to hatching period. All embryos are absent of NBT/BCIP staining. (A) 2 hpf embryo, (B) 12 hpf embryo, (C) 18 hpf embryo, (D) 24 hpf embryo, (E) 32 hpf embryo, (F) 36 hpf embryo, (G) 48 hpf embryo.

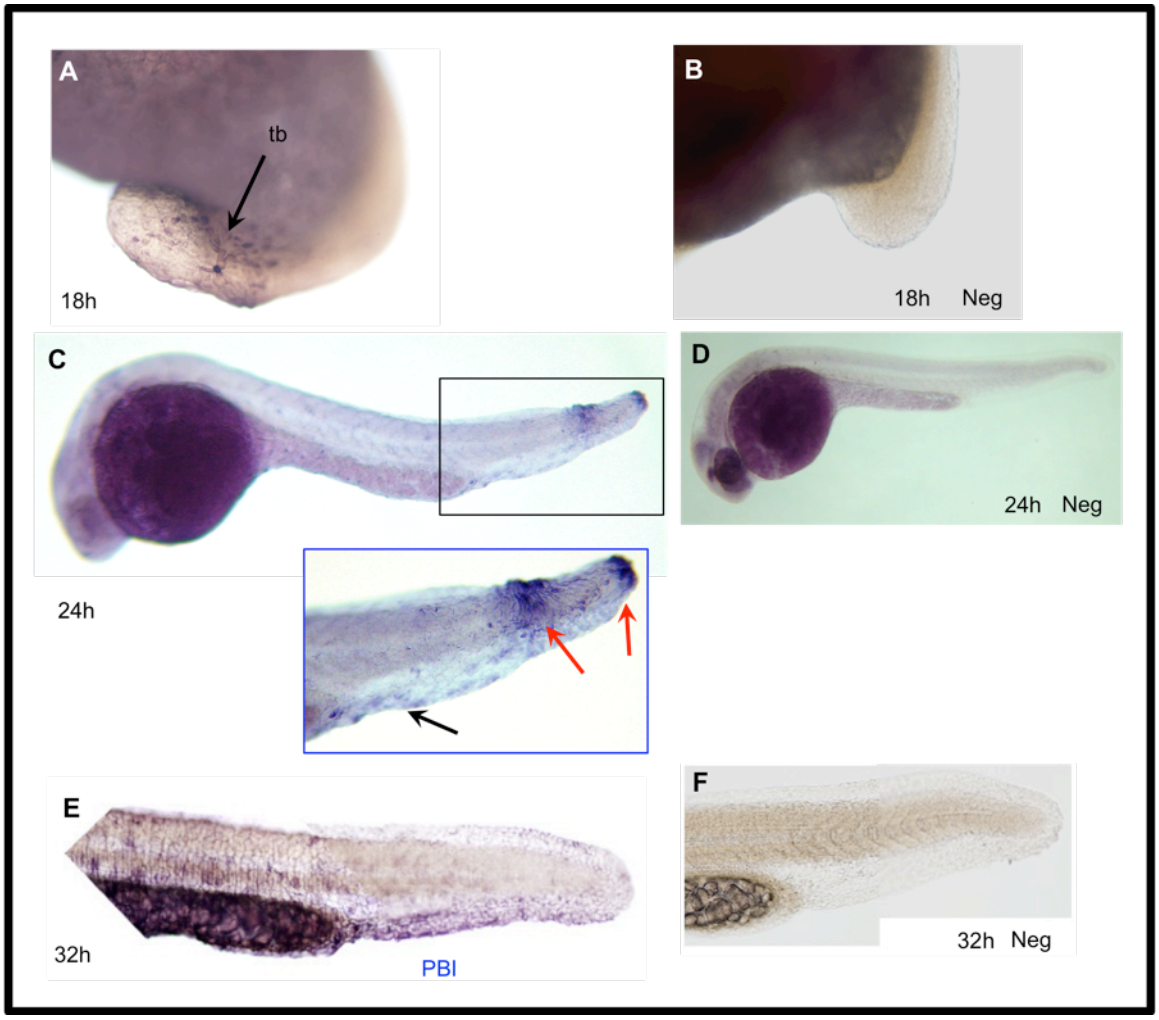

Figure 12. Whole-mount immunohistochemistry of abl expression. (A) 18 hpf embryo showing expression in the tail bud (tb), (C) 24 hpf showing expression within the posterior blood island (PBI) indicated by black arrow. Red arrows show expression within the tail, blue box shows the PBI at higher magnification. (E) 32 hpf embryo showing dark staining within the PBI, (B,D,F) Negative controls at 18, 24, and 32 hpf showing no abl expression.

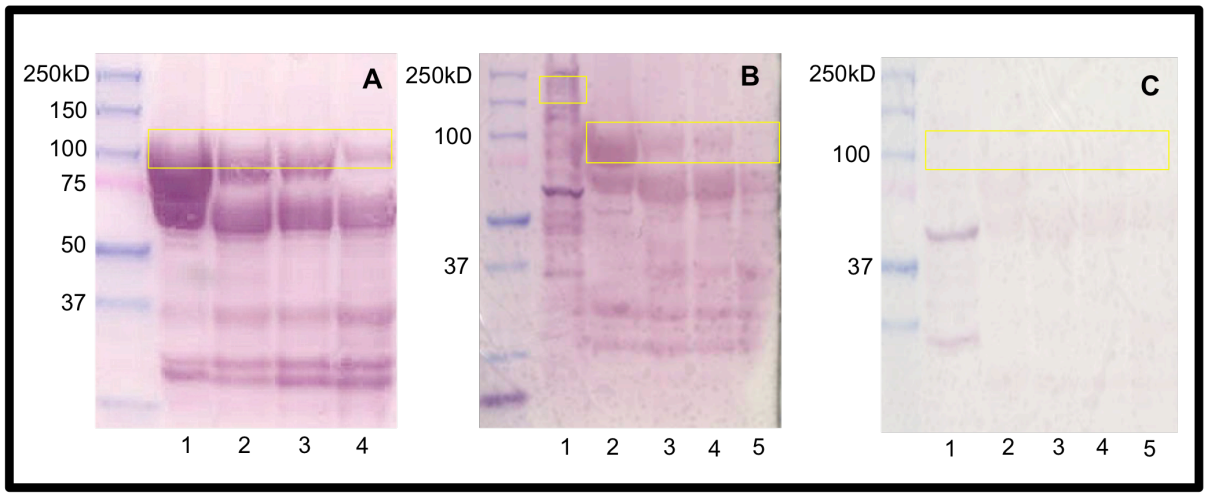

Figure 13. Western blot. Quantified protein from K562 cells and zebrafish at 18-36 hpf were used. Yellow boxes indicate bands with correct molecular weight. (A) Lane 1=18 hpf, lane 2 =24 hpf, lane 3=32 hpf, lane 4=36 hpf, (B) Lane 1=K562, lane 2=18 hpf, lane 3=24 hpf, lane 4=32 hpf, lane 5=36 hpf, (C) Pre-absorbed negative control at 4:1 ratio of peptide to antibody, lane 1=K562, lane 2=18 hpf, lane 3=24 hpf, lane 4=32 hpf, lane 5=36 hpf.

References

Agami, R., Blandino, G., Oren, M., & Shaul, Y. (1999). Interaction of c-Abl and p73 alpha and their collaboration to induce apoptosis. *Nature, 399*, 809-813.

Amar, M., Amit, M., Scoazec, J. Y., Pasquier, C., Babin-Chevaye, C., Pham Huu, T., . . . Hakim, J. (1992). K562 Cells Produce an Anti-Inflammatory Factor That Inhibits Neutrophil Functions In Vivo. *Blood, 80*, 1546-1552.

Auer, R. L., Riaz, S., & Cotter, F. E. (2007). The 13q and 11q B-cell chronic lymphocytic leukaemia-associated regions derive from a common ancestral region in the zebrafish. *British Journal of Haematology, 137*, 443-453.

Bertrand, J. Y., Kim, A. D., Violette, E. P., Stachura, D. L., Cisson, J. L., & Traver, D. (2007). Definitive hematopoiesis initiates through a committed erythromyeloid progenitor in the zebrafish embryo. *Development, 134*, 4147-4156.

Boyle, S. N., Michaud, G. A., Schweitzer, B., Predki, P. F., & Koleske, A. J. (2007). A critical role for cortactin phosphorylation by Abl-family kinases in PDGF-induced dorsal-wave formation. *Current Biology, 17*, 445-451.

Chen, J. H., Jette, C., Kanki, J. P., Aster, J., Look, A. T., & Griffin, J. D. (2006). NOTCH1-induced T-cell leukemia in transgenic zebrafish. *Blood, 108*, 1825.

Daley, G. Q., Vanetten, R. A., & Baltimore, D. (1990). Induction of chronic myelogenous leukemia in mice by the P210 BCR/ABL gene of the Philadelphia chromosome. *Science, 247*, 824-830.

Davidson, A. J., & Zon, L. I. (2004). The 'definitive' (and 'primitive') guide to zebrafish hematopoiesis. *Oncogene, 23*, 7233-7246.

Deming, P. B., Schafer, Z. T., Tashker, J. S., Potts, M. B., Deshmukh, M., & Kornbluth, S. (2004). Bcr-Abl-mediated protection from apoptosis downstream of mitochondrial cytochrome c release. *Molecular and Cellular Biology, 24*, 10289-10299.

Dereeper, A., Guignon, V., Blanc, G., Audic, S., Buffet, S., Chevenet, F., . . . Dufayard, J. F. (2008). Phylogeny.fr: robust phylogenetic analysis for the non-specialist. *Nucleic Acids Research, 36*, 465-469.

Druker, B. J. (2008). Translation of the Philadelphia chromosome into therapy for CML. *Blood, 112*, 4808-4817.

Feng, H., Langenau, D. M., Madge, J. A., Quinkertz, A., Gutierrez, A., & Neuberg, D. S. (2007). Heat-shock induction of T-cell lymphoma/leukaemia in conditional Cre/lox-regulated transgenic zebrafish. *British Journal of Haematology, 138*, 169-175.

Gong, J. G., Costanzo, A., Yang, H. Q., Melino, G., Kaelin, W. G., & Levrero, M. (1999). The tyrosine kinase c-Abl regulates p73 in apoptotic response to cisplatin-induced DNA damage. *Nature, 399*, 806-809.

Gross, A. W., & Ren, R. B. (2000). Bcr-Abl has a greater intrinsic capacity than v-Abl to induce the neoplastic expansion of myeloid cells. *Oncogene, 19*, 6286-6296.

Henkemeyer, M., West, S. R., Gertler, F. B., & Hoffmann, F. M. (1990). A novel tyrosine kinase-independent function of *Drosophila abl* correlates with proper subcellular localization. *Cell, 63*, 949-960.

Hsu, K., Traver, D., Kutok, J. L., Hagen, A., Liu, T. X., Paw, B. H., . . . Rhodes, J. (2004). The pu.1 promoter drives myeloid gene expression in zebrafish. *Blood, 104*, 1291-1297.

Huang, Y. P., Comiskey, E. O., Dupree, R. S., Li, S. X., Koleske, A. J., & Burkhardt, J. K. (2008). The c-Abl tyrosine kinase regulates actin remodeling at the immune synapse. *Blood, 112*, 111-119.

Isogai, S., Horiguchi, M., & Weinstein, B. M. (2001). The vascular anatomy of the developing zebrafish: An atlas of embryonic and early larval development. *Developmental Biology, 230*, 278-301.

Jin, H., Sood, R., Xu, J., Zhen, F., English, M. A., Liu, P. P., . . . Wen, Z. (2009). Definitive hematopoietic stem/progenitor cells manifest distinct differentiation output in the zebrafish VDA and PBI. *Development, 136*, 647-654.

Kalev-Zylinska, M. L., Horsfield, J. A., Flores, M. V. C., Postlethwait, J. H., Vitas, M. R., Baas, A. M., . . . Crosier, P. S. (2002). Runx1 is required for zebrafish blood and

vessel development and expression of a human RUNX1-CBF2T1 transgene advances a model for studies of leukemogenesis. *Development, 129*, 2015-2030.

Kimmel, C. B., Ballard, W. W., Kimmel, S. R., Ullmann, B., & Schilling, T. F. (1995). Stages of Embryonic-Development of the Zebrafish. *Developmental Dynamics, 203*, 253-310.

Koleske, A. J., Gifford, A. M., Scott, M. L., Nee, M., Bronson, R. T., Miczek, K. A., . . . Baltimore, D. (1998). Essential roles for the Abl and Arg tyrosine kinases in neurulation. *Neuron, 21*, 1259-1272.

Kurzrock, R., Kantarjian, H. M., Druker, B. J., & Talpaz, M. (2003). Philadelphia chromosome-positive leukemias: From basic mechanisms to molecular therapeutics. *Annals of Internal Medicine, 138*, 819-830.

Langenau, D. M., Traver, D., Ferrando, A. A., Kutok, J., Aster, J. C., Kanki, J. P., . . . Shuo, L. (2002). Myc-induced T-cell leukemia in transgenic zebrafish. *Blood, 100*, 110.

Lapetina, S., Mader, C. C., Machida, K., Mayer, B. J., & Koleske, A. J. (2009). Arg interacts with cortactin to promote adhesion-dependent cell edge protrusion. *Journal of Cell Biology, 185*, 503-519.

Lin, T. Y., Huang, C. H., Kao, H. H., Liou, G. G., Yeh, S. R., Cheng, C. M., . . . Pan, R. L. (2009). Abi plays an opposing role to Abl in Drosophila axonogenesis and synaptogenesis. *Development, 136*, 3099-3107.

McGahon, A. J., Brown, D. G., Martin, S. J., AmaranteMendes, G. P., Cotter, T. G., Cohen, G. M., . . . Green, D. R. (1997). Downregulation of Bcr-Abl in K562 cells restores susceptibility to apoptosis: Characterization of the apoptotic death. *Cell Death and Differentiation, 4*, 95-104.

Mebius, R. E., Miyamoto, T., Christensen, J., Domen, J., Cupedo, T., Weissman, I. L., . . . Akashi, K. (2001). The fetal liver counterpart of adult common lymphoid progenitors gives rise to all lymphoid lineages, CD45+CD4+CD3- cells, as well as macrophages. *Journal of Immunology, 166*, 6593-6601.

Meeker, N. D., & Trede, N. S. (2008). Immunology and zebrafish: Spawning new models of human disease. *Developmental and Comparative Immunology, 32*, 745-757.

Murayama, E., Kissa, K., Zapata, A., Mordelet, E., Briolat, V., Lin, H. F., . . . Handin, R. I. (2006). Tracing hematopoietic precursor migration to successive hematopoietic organs during zebrafish development. *Immunity, 25*, 963-975.

Murry, C. E., & Keller, G. (2008). Differentiation of embryonic stem cells to clinically relevant populations: Lessons from embryonic development. *Cell, 132*, 661-680.

Nowell, P. C., & Hungerford, D. A. (1960). Minute Chromosome in Human Chronic Granulocytic Leukemia. *Science, 132*, 1497-1497.

Orkin, S. H., & Zon, L. I. (2008). Hematopoiesis: An evolving paradigm for stem cell biology. *Cell, 132*, 631-644.

Parham, P. (2005). *The Immune System* (2 ed.). New York, NY: Garland Science.

Plattner, R., Kadlec, L., DeMali, K. A., Kazlauskas, A., & Pendergast, A. M. (1999). c-Abl is activated by growth factors and Src family kinases and has a role in the cellular response to PDGF. *Genes & Development, 13*, 2400-2411.

Reinhold, U., Hennig, E., Leiblein, S., Niederwieser, D., & Deininger, M. W. N. (2003). FISH for BCR-ABL on interphases of peripheral blood neutrophils but not of unselected white cells correlates with bone marrow cytogenetics in CML patients treated with imatinib. *Leukemia, 17*, 1925-1929.

Rowley, J. D. (1973). New Consistent Chromosomal Abnormality in Chronic Myelogenous Leukemia Identified by Quinacrine Fluorescence and Giemsa Staining. *Nature, 243*, 290-293.

Samokhvalov, I. M., Samokhvalova, N. I., & Nishikawa, S. (2007). Cell tracing shows the contribution of the yolk sac to adult haematopoiesis. *Nature, 446*, 1056-1061.

Sharma, V. M., Calvo, J. A., Draheim, K. M., Cunningham, L. A., Hermance, N., Beverly, L., . . . Krishnamoorthy, V. (2006). Notch1 contributes to mouse T-cell leukemia by directly inducing the expression of c-myc. *Molecular and Cellular Biology, 26*, 8022-8031.

Shtivelman, E., Lifshitz, B., Gale, R. P., & Canaani, E. (1985). Fused transcript of Abl and Bcr genes in chronic myelogenous leukemia. *Nature, 315*, 550-554.

Sipkins, D. A., Wei, X., Wu, J. W., Runnels, J. M., Cote, D., Means, T. K., . . . Luster, A. D. (2005). In vivo imaging of specialized bone marrow endothelial microdomains for tumour engraftment. *Nature, 435*, 969-973.

Sirvent, A., Benistant, C., & Roche, S. (2008). Cytoplasmic signalling by the c-Abl tyrosine kinase in normal and cancer cells. *Biology of the Cell, 100*, 617-631.

Srinivasan, D., & Plattner, R. (2006). Activation of Abl tyrosine kinases promotes invasion of aggressive breast cancer cells. *Cancer Research, 66*, 5648-5655.

Srinivasan, D., Sims, J. T., & Plattner, R. (2008). Aggressive breast cancer cells are dependent on activated Abl kinases for proliferation, anchorage-independent growth and survival. *Oncogene, 27*, 1095-1105.

Stevens, T. L., Rogers, E. M., Koontz, L. M., Fox, D. T., Homem, C. C. F., Nowotarski, S. H., . . . Artabazon, N. B. (2008). Using Bcr-Abl to examine mechanisms by which Abl kinase regulates morphogenesis in Drosophila. *Molecular Biology of the Cell, 19*, 378-393.

Sun, X. G., Majumder, P., Shioya, H., Wu, F., Kumar, S., Weichselbaum, R., . . . Kharbanda, S. (2000). Activation of the cytoplasmic c-Abl tyrosine kinase by reactive oxygen species. *Journal of Biological Chemistry, 275*, 17237-17240.

Thisse, C., & Thisse, B. (2008). High-resolution in situ hybridization to whole-mount zebrafish embryos. *Nature Protocols, 3*, 59-69.

Tzeng, S. J., Bolland, S., Inabe, K., Kurosaki, T., & Pierce, S. K. (2005). The B cell inhibitory Fc receptor triggers apoptosis by a novel c-Abl family kinase-dependent pathway. *Journal of Biological Chemistry, 280*, 35247-35254.

Ward, A. C., McPhee, D. O., Condron, M. M., Varma, S., Cody, S. H., Onnebo, S. M., . . . Paw, B. H. (2003). The zebrafish spi1 promoter drives myeloid-specific expression in stable transgenic fish. *Blood, 102*, 3238-3240.

Weissman, I. L., Papaioannou, V., & Gardern, R.L. (1978). *Fetal hematopoietic origins of the adult hematolymphoid system*. Plainview, NY: Cold Spring Harbor Laboratory press.

Wetzler, M., Talpaz, M., Van Etten, R. A., Hirsh-Ginsberg, C., Beran, M., & Kurzrock, R. (1993). Subcellular localization of Bcr, Abl, and Bcr-Abl proteins in normal and leukemic cells and correlation of expression with myeloid differentiation. *Journal of Clinical Investigation, 92*, 1925-1939.

Willett, C. E., Cortes, A., Zuasti, A., & Zapata, A. G. (1999). Early hematopoiesis and developing lymphoid organs in the zebrafish. *Developmental Dynamics, 214*, 323-336.

Yoder, J. A., Nielsen, M. E., Amemiya, C. T., & Litman, G. W. (2002). Zebrafish as an immunological model system. *Microbes and Infection, 4*, 1469-1478.

Yoshihara, H., Arai, F., Hosokawa, K., Hagiwara, T., Takubo, K., Nakamura, Y., . . . Gomei, Y. (2007). Thrombopoietin/MPL signaling regulates hematopoietic stem cell quiescence and interaction with the osteoblastic niche. *Cell Stem Cell, 1*, 685-697.

Zapata, A., Diez, B., Cejalvo, T., Frias, C. G., & Cortes, A. (2006). Ontogeny of the immune system of fish. *Fish & Shellfish Immunology, 20*, 126-136.

Zhuravleva, J., Paggetti, J., Martin, L., Hammann, A., Solary, E., Bastie, J. N., . . . Delva, L. (2008). MOZ/TIF2-induced acute myeloid leukaemia in transgenic fish. *British Journal of Haematology, 143*, 378-382.

Zipfel, P. A., Zhang, W. G., Quiroz, M., & Pendergast, A. M. (2004). Requirement for Abl kinases in T cell receptor signaling. *Current Biology, 14*, 1222-1231.

BIOGRAPHICAL SKETCH

Born the first of three sons to Richard and Nora de Triquet on August 5th, 1986 at Ft. Belvoir, Virginia, Ricky de Triquet has spent much of his life traveling. With a father in the Marines, he was afforded the experience of multiple cross-country drives and trans-pacific flights before ten years of age. The hardwood forests of the Pacific Northwest, the jungles of Southeast Asia, the chaparral of the southern California, and the peanut farms of Suffolk, Virginia name just a few of his homes. This myriad of locales gives him a rare perspective of the globe's diverse cultures, cuisine, and ecosystems that he is forever grateful for. Ricky attended Belmont Abbey College where he joined the men's varsity soccer team and earned a Bachelor of Science in Biology.

His graduate research, involving a cancer causing protein, is an inherent interest of his born by personal experiences; he hopes that publication will add to the current momentum in favor of cancer therapy. At this stage in his career, he looks toward the future to continue his education in many areas, not just science, and knows that he will be a lifelong learner.